

COMBINED FREE AND FORCED CONVECTION IN A HORIZONTAL TUBE
UNDER UNIFORM HEAT FLUX

by

ARTHUR K. KUPPER

dipl. Ing. ETH 1964

A THESIS SUBMITTED IN PARTIAL FULFILMENT OF
THE REQUIREMENTS FOR THE DEGREE OF
M.A.Sc.

in the Department
of
Mechanical Engineering

We accept this thesis as conforming to the
required standard

THE UNIVERSITY OF BRITISH COLUMBIA

October 1968

In presenting this thesis in partial fulfilment of the requirements for an advanced degree at the University of British Columbia, I agree that the Library shall make it freely available for reference and study. I further agree that permission for extensive copying of this thesis for scholarly purposes may be granted by the Head of my Department or by his representatives. It is understood that copying or publication of this thesis for financial gain shall not be allowed without my written permission.

Department of MECH. ENGR.

The University of British Columbia
Vancouver 8, Canada

Date 12-21-68

ABSTRACT

This thesis presents experimental results of combined free and forced convection laminar heat transfer for water flowing through a circular horizontal tube with uniform wall heat flux. The Reynolds number ranged from 100 to 2000, and changes in heat transfer rate allowed a variation of Grashof number from 300 to 30,000. The Prandtl number ranged from 4 to 9. The effect of secondary flow created by free convection occurring at higher Grashof number indicates an increase in Nusselt number up to 200 per cent. For the fully-developed region two tentative correlations are given. The expression

$$Nu = 48/11 + 0.047 Pr^{1/3} (Re Ra)^{1/5}$$

correlates 53 per cent of the data to within ± 10 per cent. Another slightly more accurate expression which correlates 68 per cent of the data to within ± 10 per cent, but does not satisfy the pure forced convection, is

$$Nu = 2.41 + 0.082 Pr^{1/3} (Re Ra)^{1/5}$$

ACKNOWLEDGEMENTS

I wish to express my deep gratitude to Dr. M. Iqbal and to Dr. E.G. Hauptmann for their guidance and advice throughout my graduate studies. Also, I wish to thank the members of the Mechanical Engineering Department staff for their assistance and the Department for the use of its facilities. The financial assistance given by the University of British Columbia and by the National Research Council of Canada is gratefully acknowledged.

TABLE OF CONTENTS

ABSTRACT	ii
ACKNOWLEDGEMENT	iii
LIST OF FIGURES	vi
NOMENCLATURE	viii
INTRODUCTION	1
LITERATURE SURVEY	4
Uniform Wall Temperature	5
Uniform Wall Heat Flux	9
PURPOSE OF EXPERIMENT	19
DESCRIPTION OF EXPERIMENTAL EQUIPMENT	19
Flow Loop	19
Test Section	21
Test Section Insulation	25
Power Supply	27
Temperature Measurement	27
EXPERIMENTAL PROCEDURE	29
Test Procedure	29
Thermocouple Calibration Method	29
Calibration Result	30
RESULTS AND DISCUSSION	31
Entrance Length and Circumferential Temperature Variation	32
Axial Temperature Profiles	35

Contents continued

Local Nusselt Number	38
Heat Transfer Correlation	47
CONCLUSION	51
REFERENCES	52
APPENDIX A DERIVATION OF GOVERNING EQUATIONS	55
APPENDIX B LOCATION OF TEST SECTION THERMOCOUPLES	56
APPENDIX C SAMPLE CALCULATION	58
APPENDIX D ERROR ANALYSIS	62
APPENDIX E TABULATED LOCAL HEAT TRANSFER DATA	65

LIST OF FIGURES

1a	Velocity Profiles for Heated upward Flow	3
1b	Motion of Fluid Particles under Buoyancy Effects	3
2	Coordinate System	4
3	Temperature Variation in the Axial Direction	6
4	Reproduction of Figure 1 from Reference 14	12
5	Reproduction of Figure 3 from Reference 14	13
6	Reproduction of Figure 4 from Reference 14	13
7	Reproduction of Figure 9 from Reference 16	15
8	Reproduction of Figure 6 from Reference 18	17
9	Schematic of Heat Transfer Loop	20
10	Partial View of Experimental Arrangement	22
11	View of Test Section	23
12	Thermocouple Placing on Test Section Circumference	24
13	Schematic of Power Supply	26
14	Thermocouple Circuit	28
15	Representative Temperature Profile, Run Number 3	33
16	Representative Temperature Profile, Run Number 42	34
17	Representative Temperature Profile, Run Number 1	36
18	Representative Temperature Profile, Run Number 43	37
19	Representative Temperature Profile, Run Number 37	39

List of Figures continued

20	Representative Temperature Profile, Run Number 27	40
21	Representative Nusselt Number Profile, Run Number 3	41
22	Representative Nusselt Number Profile, Run Number 37	43
23	Representative Nusselt Number Profile, Run Number 1	44
24	Representative Nusselt Number Profile, Run Number 43	45
25	Representative Nusselt Number Profiles, Run Numbers 1 and 43	46
26	Correlation of Nusselt Number, Equation 17	48
27	Correlation of Nusselt Number, Equation 18	49

NOMENCLATURE

A	Axial temperature gradient
a	Tube radius
C	Axial pressure gradient in fluid
c_p	Specific heat at constant pressure
D	Tube diameter
E	Voltage
Gr	$\frac{\beta g \Delta T D^3}{\nu^2}$, Grashof number
Gz	$\frac{\pi}{4} \text{Re} \text{Pr} \frac{L_1}{L_2}$, Graetz number
g	Acceleration of gravity
h	$\frac{q}{T_w - T}$, heat transfer coefficient
k	Thermal conductivity
L	Characteristic length
\dot{m}	Mass flow rate
Nu	$\frac{hD}{k}$, Nusselt number
P	Power input
Pr	$\frac{c_p \mu}{k}$, Prandtl number
q	Wall heat flux density
R	Dimensionless radial coordinate

Nomenclature continued

r	Radial coordinate
Ra	$Gr Pr$, Rayleigh number
Re	$\frac{\bar{u} D}{\nu}$, Reynolds number
T	Fluid bulk temperature
T_w	Tube temperature
T^*	Dimensionless temperature
\bar{u}	Average velocity
V_x	Dimensionless axial velocity
v_r	Velocity in radial direction
v_θ	Velocity in angular direction
X	Coordinate in axial direction
α	Tube inclination with respect to the horizontal position
β	Expansion coefficient
ΔT	Temperature difference, fluid bulk to wall
∇^2	Laplacian
θ	Angular coordinate
μ	Dynamic viscosity of fluid
ν	Kinematic viscosity of fluid
ρ	Density of fluid
ψ	Stokes stream function

INTRODUCTION

The rate of heat transfer between a solid surface and a fluid may depend on both free and forced convection mechanisms. Forced convection occurs when fluid motion is produced by a pump or similar means. In free or natural convection, fluid motion occurs due to buoyancy forces produced from temperature (or equivalently density) differences arising from the heat transfer situation itself. For laminar heat transfer associated with a circular tube, the buoyancy forces are characterized by the dimensionless Grashof number, and the forced flow is characterized by the Reynolds number. In most physical situations, both modes of heat transfer are present, and their relative magnitude determines whether a flow is considered as forced, free, or combined free and forced convection. The present investigation originates from study of flow and heat transfer through tubes of flat plate solar collectors, where both free and forced convection mechanisms are important.

In practice, pure forced convection is never exactly realized, and use of the term merely implies that free convection effects are negligible. Where natural convection effects are not negligible, the solid surface orientation with respect to the direction of gravitational force also becomes important.

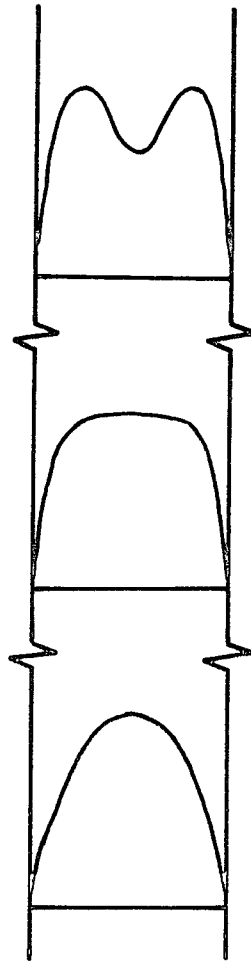
For heating of upward flow in vertical tubes, free convection aids the forced upward motion of fluid near the wall. This creates steeper velocity and temperature gradients near the wall and hence results in a higher heat transfer coefficient. To satisfy continuity, the increased velocity near the wall results in flow retardation at the tube centre,

and in extreme cases a reversal of flow at the tube centre may even occur (Fig. 1a).

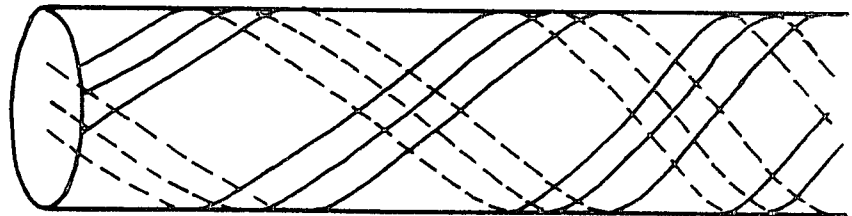
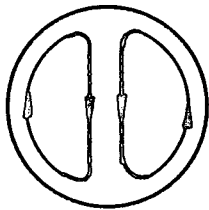
Free convection opposes the forced flow during heating of fluids flowing downward, and a decrease in heat transfer rate results.

In the case of a horizontal tube, the free and forced convective motions are perpendicular to one another. For pure forced flow the velocity profile is symmetrical with respect to the tube axis. However, when the tube wall is heated, the fluid particles receive heat from the wall, forming a temperature gradient through the fluid. The fluid particles near the wall have a lower density (in most fluids) than those in the centre of the tube, and motion is created because of gravity forces. The fluid particles near the wall rise upwards, while those in the centre move downwards. Superimposing this motion on forced flow, the fluid particles develop spiral trajectories, ascending near the wall toward the top and descending in the centre as they move through the tube (Fig. 1b).

There are many possible variations of the problem stated. The fluid may be cooled or heated from the tube wall in different ways. In addition, internal heat sources may also be present. The two most interesting and practical cases of combined free and forced convection in horizontal tubes occur when either the wall temperature or wall heat flux are approximately uniform. The present investigation deals with the latter case.



(1A)



(1B)

FIGURE 1A VELOCITY PROFILES FOR HEATED UPWARD FLOW

1B MOTION OF FLUID PARTICLES UNDER BUOYANCY EFFECTS

LITERATURE SURVEY

Forced convection is independent of tube orientation and has been extensively investigated. The influence of free convection on forced flow in horizontal tubes has been given somewhat less attention. Five equations govern the temperature and velocity fields in this problem. The continuity equation, the momentum equations (one for each of the three velocity components) and the energy equation. Using cylindrical coordinates, as outlined in Fig. 2, and nondimensional forms Iqbal and Stachiewicz [12]* obtained for angles α other than 90° ,

$$\nabla^4 \psi + \frac{1}{R} \left\{ \frac{\partial \psi}{\partial R} \frac{\partial}{\partial \theta} - \frac{\partial \psi}{\partial \theta} \frac{\partial}{\partial R} \right\} \nabla^2 \psi = Ra \left\{ \frac{\partial T^*}{\partial R} \sin \theta + \frac{1}{R} \frac{\partial T^*}{\partial \theta} \cos \theta \right\} \cos \alpha \quad (1)$$

$$\nabla^2 V_x + \frac{1}{R} \left\{ \frac{\partial \psi}{\partial R} \frac{\partial}{\partial \theta} - \frac{\partial \psi}{\partial \theta} \frac{\partial}{\partial R} \right\} V_x + 4Re - RaT^* \sin \alpha = 0 \quad (2)$$

$$\nabla^2 T^* + \frac{Pr}{R} \left\{ \frac{\partial \psi}{\partial R} \frac{\partial}{\partial \theta} - \frac{\partial \psi}{\partial \theta} \frac{\partial}{\partial R} \right\} T^* + V_x = 0 \quad (3)$$

The derivation of the above equations is explained in Appendix A.

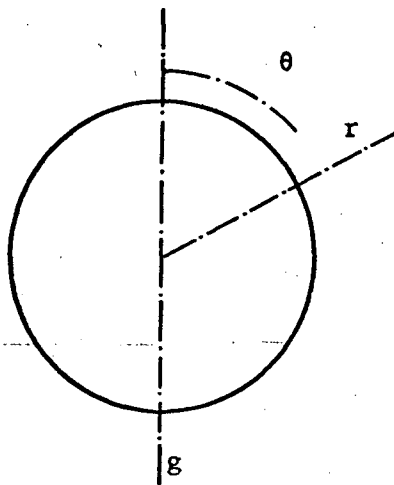


FIGURE 2 Coordinate System

* Numbers in square brackets refer to references.

In the above equation physical properties of the fluid are considered constant except for density variation affecting the buoyancy terms. In the energy equation, axial conduction, viscous dissipation and pressure work terms have been ignored. Furthermore, the flow is considered hydrodynamically fully-developed.

Two boundary conditions for the temperature at the wall are usually encountered in most practical instances of laminar heat transfer in circular horizontal tubes: uniform wall temperature (such as arising from heating with a condensing vapor), and uniform wall heat flux (such as arising from heating with electric currents). These two boundary conditions produce axial temperature variations as shown in Fig. 3.

a) Uniform Wall Temperature

Apparently no theoretical study has yet been made for combined free and forced convection in horizontal tubes with constant wall temperature. There are, however, several reports regarding experimental investigations.

Colburn [1] has shown that natural convection may increase the rate of heat transfer by a factor of three or four. He presented the relationship

$$Nu_{am} = 1.75 Gz^{1/3} (1 + 0.015 Gr_f^{1/3}) (\mu_b/\mu_f)^{1/3} \quad (4)$$

where Nu_{am} is the Nusselt number with fluid properties based on the arithmetic mean temperature difference between fluid and tube (the indices "f" and "b" refer to film and bulk temperature respectively). The correction factor $(1 + 0.015 Gr_f^{1/3}) (\mu_b/\mu_f)^{1/3}$ allows for both natural convection

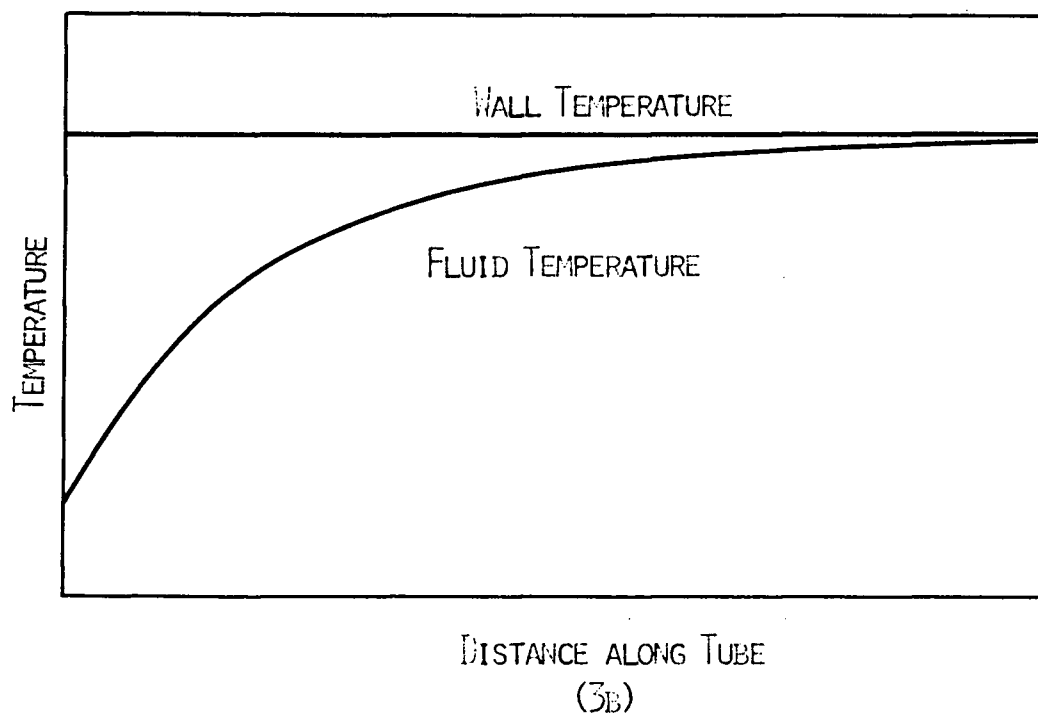
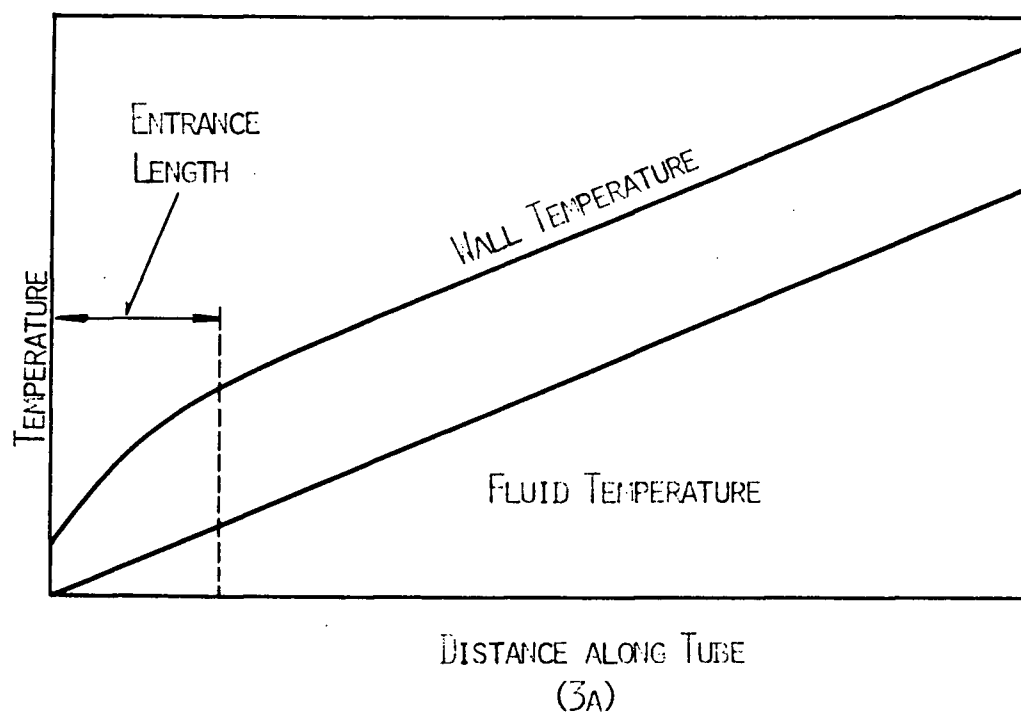


FIGURE 3 TEMPERATURE VARIATION IN THE AXIAL DIRECTION

3A CONSTANT WALL HEAT FLUX

3B CONSTANT WALL TEMPERATURE

and radial variation of fluid properties.

Sieder and Tate [2] suggested that the viscosity variation in equation (4) might be replaced by $(\mu_b/\mu_w)^{0.14}$, where μ_w denotes the fluid viscosity evaluated at the wall temperature. They also suggested the Grashof number should be evaluated at the mean fluid temperature rather than film temperature. However, these changes throw no further light on the natural convection process itself.

From their extensive experimental data, Kern and Othmer [3] noticed that Sieder and Tate's [2] equation predicted high heat transfer coefficients at high Reynolds numbers, and the opposite at low Reynolds numbers. For this reason they introduced an arbitrary function $(\ln_{10} Re)^{-1}$ in the natural convection term, obtaining the equation

$$Nu_{am} = 1.86 \left\{ \left(\frac{DG}{\mu_m} \right) \left(\frac{cp\mu}{k} \right) \left(\frac{D}{L} \right) \right\}^{1/3} \frac{2.25 (1 + 0.01 Gr_m^{1/3})}{\ln_{10} Re} \left(\frac{\mu_b}{\mu_w} \right)^{0.14} \quad (5)$$

Kern and Othmer obtained markedly better correlation of their results with this equation, than by using the preceeding equations.

Martinelli et al. [4] presented a theoretical approach to the problem of combined forced and free convection. The analysis applied to the cases of heating of fluids flowing vertically upwards, and cooling of fluids flowing downwards in tubes with uniform wall temperature. They obtained the equation

$$Nu_{am} = 1.75 F_1 \left\{ Gz_m + 0.0722 F_2 \left(\frac{Gr_w Pr_w D}{L} \right)^{0.75} \right\}^{1/3} \quad (6)$$

The correction factor F_1 allows for use of arithmetic rather than loga-

rithmic mean temperature differences, while the correction factor F_2 allows for a reduction in free convection forces as the fluid bulk temperature rises.

From data for heating of oils in horizontal tubes, Eubank and Proctor [5] modified equation (6) to the form

$$Nu_{am} = 1.75 \left\{ Gz_m + 12.6 \left(\frac{Gr_m Pr_m D}{L} \right)^{0.40} \right\}^{1/3} \left(\frac{\mu_b}{\mu_w} \right)^{0.14} \quad (7)$$

The Grashof number is now based on mean temperature difference between the wall and fluid, and the properties of the fluid are based on the mean bulk temperature.

McAdams [6] recommended an equation similar to that presented by Eubank and Proctor [5], except with the coefficients 12.6 and 0.4 replaced by 0.04 and 0.75 respectively.

Jackson, Spurlock, and Purdy [7] have studied heat transfer rates using air in a constant temperature horizontal tube. Their results are well represented by the semi-theoretical equation

$$Nu_{lm} = 2.67 \left\{ Gz_m^2 + 0.0087^2 (Gr_w Pr_w)^{1.5} \right\}^{1/6} \quad (8)$$

The subscript "lm" denotes that the heat transfer coefficient is based on logarithmic mean temperature difference.

Oliver [8] reported an investigation of the same problem using relatively non-viscous liquids. He presented the following relationship

$$Nu_{am} = 1.75 \left\{ Gz + 5.6 \cdot 10^{-4} (Gr_m Pr_m \frac{L}{D})^{0.7} \right\}^{1/3} (\mu_w / \mu_b)^{-0.14} \quad (9)$$

It should be noted that the ratio L/D rather than D/L is used. The reason is that when the Grashof number is multiplied by the D/L ratio, a term D^4 occurs, with the result that a small variation in D produces large variations in $(Gr Pr \frac{D}{L})$. This variation is not reflected by corresponding changes in heat transfer coefficients.

Brown and Thomas [9] conducted a study of combined free and forced convection heat transfer in horizontal tubes, and proposed the relation

$$Nu (\mu_w / \mu_b)^{0.14} = 1.75 \{ Gz + 0.012 (Gz Gr^{1/3})^{4/3} \}^{1/3} \quad (10)$$

However, their results do not agree with existing correlations.

Martin and Carmichael [10] have also reported results for local heat transfer coefficients for this problem, using water as the heat transfer medium.

b) Uniform Wall Heat Flux

Very few theoretical analyses are available for combined free and forced convection in a horizontal tube under uniform heat flux.

Morton [11] analysed the problem by solving equations (1) to (3) by a perturbation method, using the Rayleigh number as a perturbation parameter. The Nusselt number based on the mean temperature was evaluated from the resulting distributions and was expressed by the following asymptotic expression valid for small values of Ra , Re and Pr

$$Nu = 6 \{ 1 + (0.0586 - 0.0852 Pr + 0.2686 Pr^2) \left(\frac{Ra Re}{4608} \right)^2 + \dots \} \quad (11)$$

The mean temperature was defined as $T_m = \int T dA / A$. No numerical limits

of Rayleigh number were given for the region of validity of the results.

Iqbal and Stachiewicz [12] analyzed the problem including the effect of tube orientation. They also solved equation (1) - (3) by a perturbation method using the Rayleigh number as a perturbation parameter. However, the Nusselt number was based on the bulk temperature, defined as

$$T_b = \int T v \, dA / \int v \, dA \quad (12)$$

They have shown that for horizontal tubes, the Nusselt number based on equation (12) is a function of the product $RaRe$ as well as Pr , while for flow through inclined tubes $Nu = f(Re, Ra, Pr)$. It is known [20] that for flow through vertical tubes, $Nu = f(Ra)$ only.

Another theoretical investigation of combined free and forced convection in horizontal tubes with uniform heat flux was reported by Del Casal and Gill [13]. In their analysis they assumed the fluid properties constant, except that density was allowed to vary throughout the governing equations. The governing equations were also solved by perturbation analysis, the ratio Gr/Re^2 being used as perturbation parameter. Del Casal and Gill state that the Froude number, characterizing density differences, also enters the problem. However, no solution for the energy equation or Nusselt number was given.

There are few experimental investigations available in the literature for the case of combined free and forced convection in horizontal tubes under uniform heat flux.

Ede [14] carried out an experiment using seven different tube diam-

eters, with both air and water used as the heat transfer medium. Reynolds numbers were varied from 300 to 100,000, while Grashof number varied up to 10^7 . The Prandtl number was approximately 0.7 for air, and varied from 4 - 12 for water. Ede plotted his results in three different ways, and his figures are reproduced in Figs. 4 to 6. Unfortunately, no mention of the values of Grashof number employed at various Reynolds numbers was made. Ede also presented an empirical correlation for the Nusselt number as

$$Nu = 4.36 (1 + 0.06 Gr^{0.3}) \quad (13)$$

Considering the theoretical studies of combined free and forced convection in horizontal tubes, one notices the lack of parameters such as Prandtl number and Reynolds number in Ede's correlation.

McComas and Eckert [15] reported an experimental study on combined free and forced convection heat transfer under uniform wall heat flux in a horizontal tube. Air was used as heat transfer medium. The Grashof number was varied by using air at different pressures. It ranged from 1 to 1000. McComas and Eckert did not present any working correlation, on the grounds that insufficient experimental data was available for this situation.

Recently, a report was published by Mori et al. [16] on free and forced convection in horizontal tubes with constant wall heat flux, using air as a heat transfer medium. Measurements of temperature and velocity distribution at certain cross sections of the test tube were made, and the local Nusselt number was calculated from local wall temperature. The

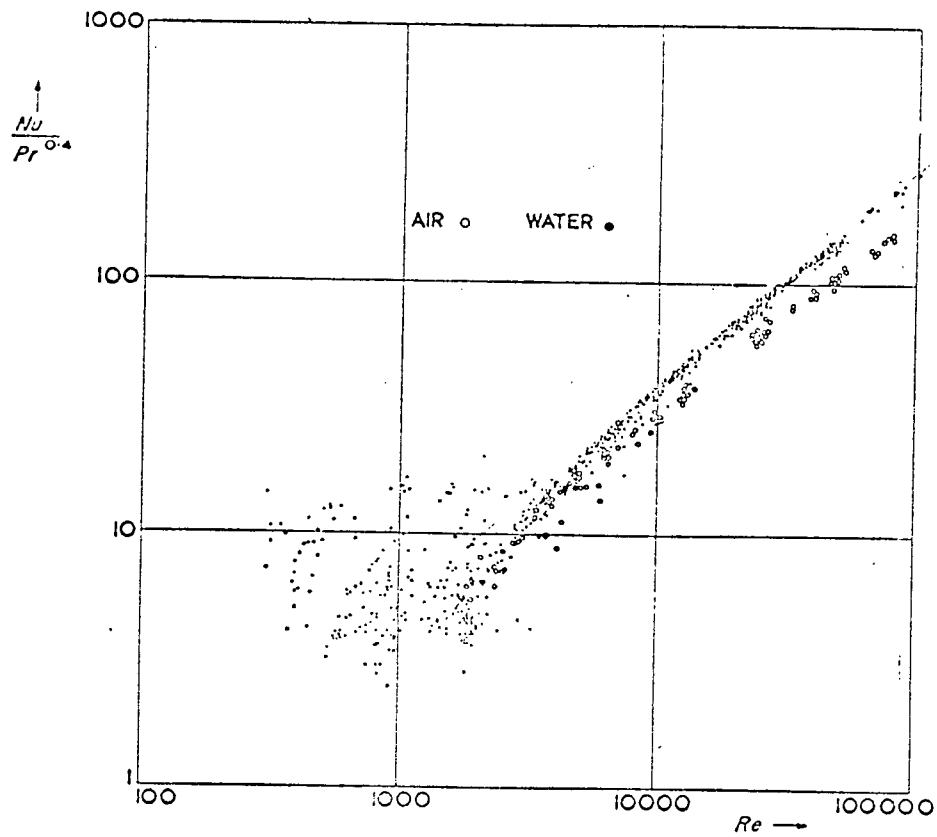


FIGURE 4 REPRODUCTION OF FIGURE 1 FROM REFERENCE 14

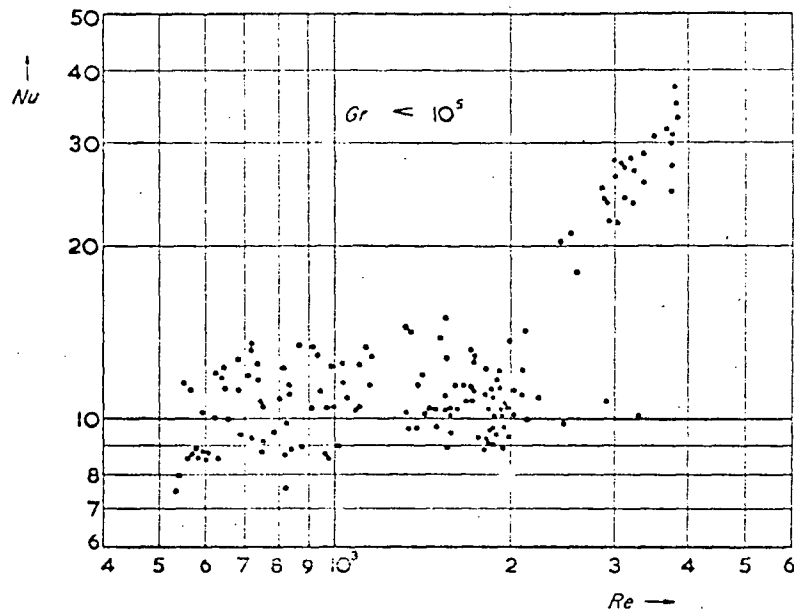


FIGURE 5 REPRODUCTION OF FIGURE 3 FROM REFERENCE 14

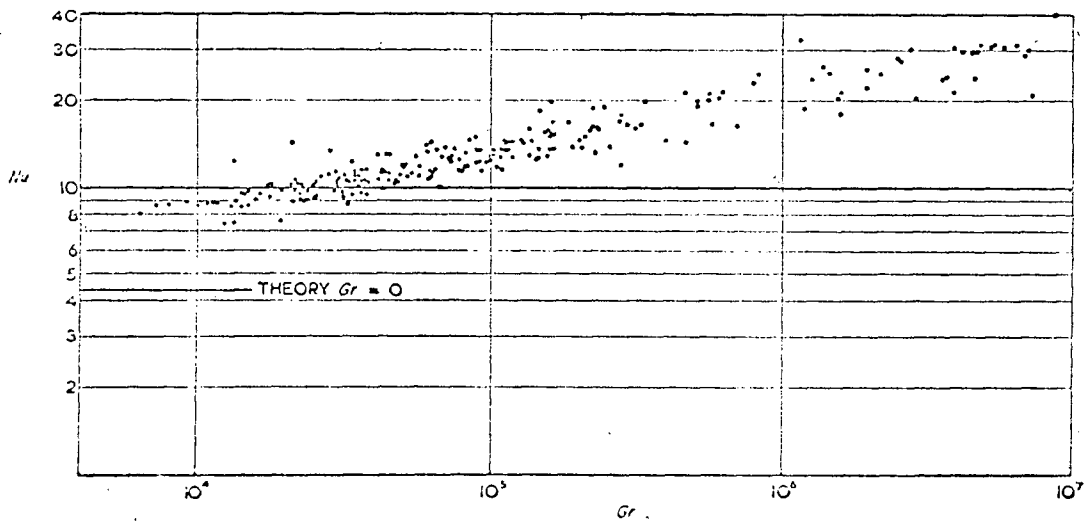


FIGURE 6 REPRODUCTION OF FIGURE 4 FROM REFERENCE 14

Reynolds number was varied from 100 to 130,000. The Nusselt number correlation was expressed by the relation

$$Nu = 0.61 (ReRa)^{1/5} \left\{ 1 + \frac{1.8}{(Re Ra)^{1/5}} \right\} \quad (14)$$

which represents curve 2 of Fig. 7. It remains to be explained why this form of correlation was chosen, since one notices that equation (14) is equivalent to

$$Nu = 1.098 + 0.61 (Re Ra)^{1/5} \quad (14a)$$

Although Morton's analysis shows that Nusselt number is a function of the $RaRe$ product, as well as Pr , Mori's equation does not contain the Prandtl number explicitly. The reason for this appears to be due to the fact that Mori used only air ($Pr \approx 1$) in his experimental investigation and therefore no correlation with Pr could be attempted.

In a second report, Mori and Futagami [17] present a theoretical investigation of the same problem. In their analysis they divide the flow in the tube into a thin layer along the tube wall and a core region. In the thin layer, the velocity and temperature fields are affected by viscosity and thermal conductivity. On the other hand, in the core region, the velocity and temperature fields are affected mainly by the secondary flow and the effects of viscosity and thermal conductivity are disregarded. They give an approximate solution for very large products of $ReRa$, and expressed the Nusselt number as

$$\frac{Nu}{Nu_o} = 0.2189 \frac{(Re Ra)^{1/5}}{\left(\frac{1}{\zeta_m} + \frac{1}{10 Pr} \right) \zeta_m^{2/5}} \quad (15)$$

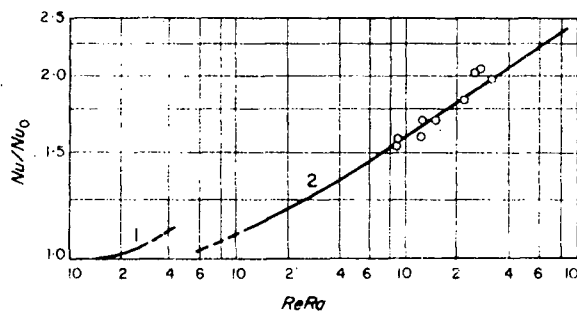


FIG. 9. (Nu/Nu_0) $Re Ra$ diagram (laminar flow).

FIGURE 7 REPRODUCTION OF FIGURE 9 FROM REFERENCE 16

where $Nu_0 = 48/11$ and ζ_m is given by

$$10\zeta_m^6 + 5\zeta_m^3 Pr - (25 Pr + 4)\zeta_m^2 Pr + (20 Pr + 1)\zeta_m Pr - 5 Pr^2 = 0$$

Very recently Shannon and Depew [18] published an experimental investigation of flow through a horizontal circular tube with uniform wall heat flux. Water near the ice point was used as heat transfer medium. The Reynolds number was varied from 120 to 2300, and the Grashof number ranged up to $2.5 \cdot 10^5$. No correlation formula was given, but they plotted their data as $(Nu - Nu_{Gz})$ versus $(Gr Pr)^{1/4} / Nu_{Gz}$ as shown in Fig. 8. Nu is the Nusselt number measured in their experiment, and Nu_{Gz} is a function of Graetz number evaluated from Siegel's [19] solution. Their difference represents the portion of Nusselt number which is due to free convection. It was felt that the natural convection is dependent on the term $(Gr Pr)^{1/4}$ only, as suggested by Mikesell [21].

In the entrance region, the heat transfer rate depends on the ratio L/D , which can be taken into account by introducing the Graetz number. For the fully developed flow region however, the heat transfer coefficient will be independent of the tube length, and hence the Nusselt number will not be a function of the Graetz number.

Table 1 gives a summary of the region of dimensionless parameters covered by experimental data reported by references [14] - [18]. It also contains the region covered by the present investigation.

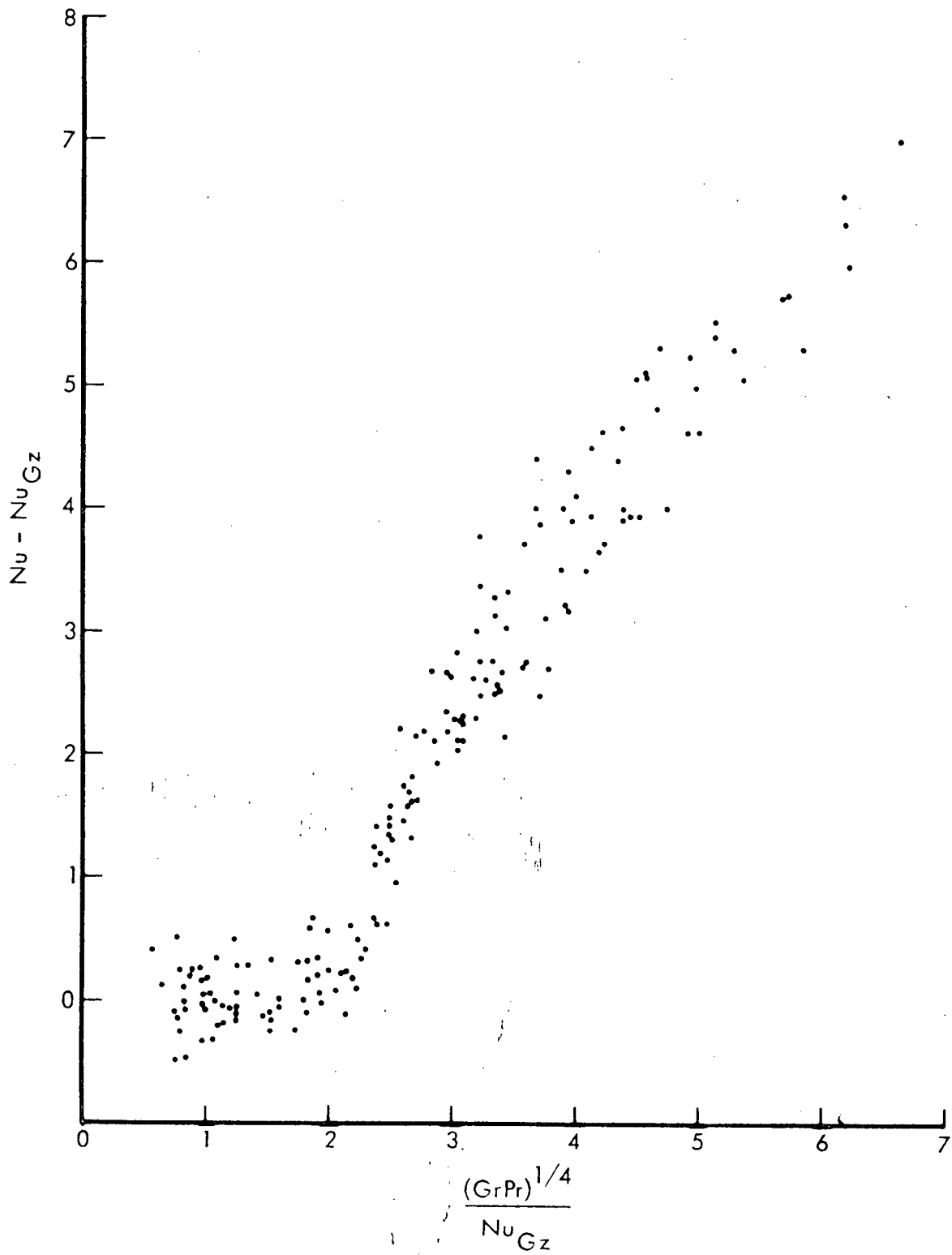


FIGURE 8 REPRODUCTION OF FIGURE 6 FROM REFERENCE 18

	Re	Gr	Pr	Fluid
Ede	300 - 100,000	---	---	Air / Water
McComas & Eckert	100 - 900	1 - 1,000	0.75	Air
Mori	1,890 - 1,450	33 - 57	0.75	Air
Shannon & Depew	120 - 2,300	up to $2.5 \cdot 10^5$	2 - 14	Water
Present Investigation	100 - 2,000	300 - 30,000	4 - 9	Water

TABLE 1 Summary of Experimental Investigations.

PURPOSE OF EXPERIMENT

As mentioned in the last chapter, the purpose of the present experiment was to obtain the heat transfer coefficient, or Nusselt number, as a function of other dimensionless parameters. The apparatus was also designed to investigate the entrance length required for the flow to become fully-developed.

DESCRIPTION OF EXPERIMENTAL EQUIPMENT

Flow Loop

A schematic diagram of the flow loop is shown in Fig. 9. The heat transfer medium used was distilled and deionized water. A constant temperature bath was used to maintain a steady inlet temperature. It also provided a constant head of eight feet, assuring a constant flow rate. Water from the head tank flowed down the stand pipe, and temperature was measured before entering the test section. It then passed through a smooth inlet to the hydrodynamic approach, then into the test section and to the outlet. The inlet, tube, and outlet were placed in a vacuum tube for heat insulation. The hydrodynamic approach section has a length of one foot and an outside diameter of 0.25 inch. The length to diameter ratio of 52 allowed the velocity profile to become fully-developed.

The six foot long test section was separated thermally from the hydrodynamic approach section by a teflon disk. The hydrodynamic approach and test section are both from the same 10/1000 inch wall thick-

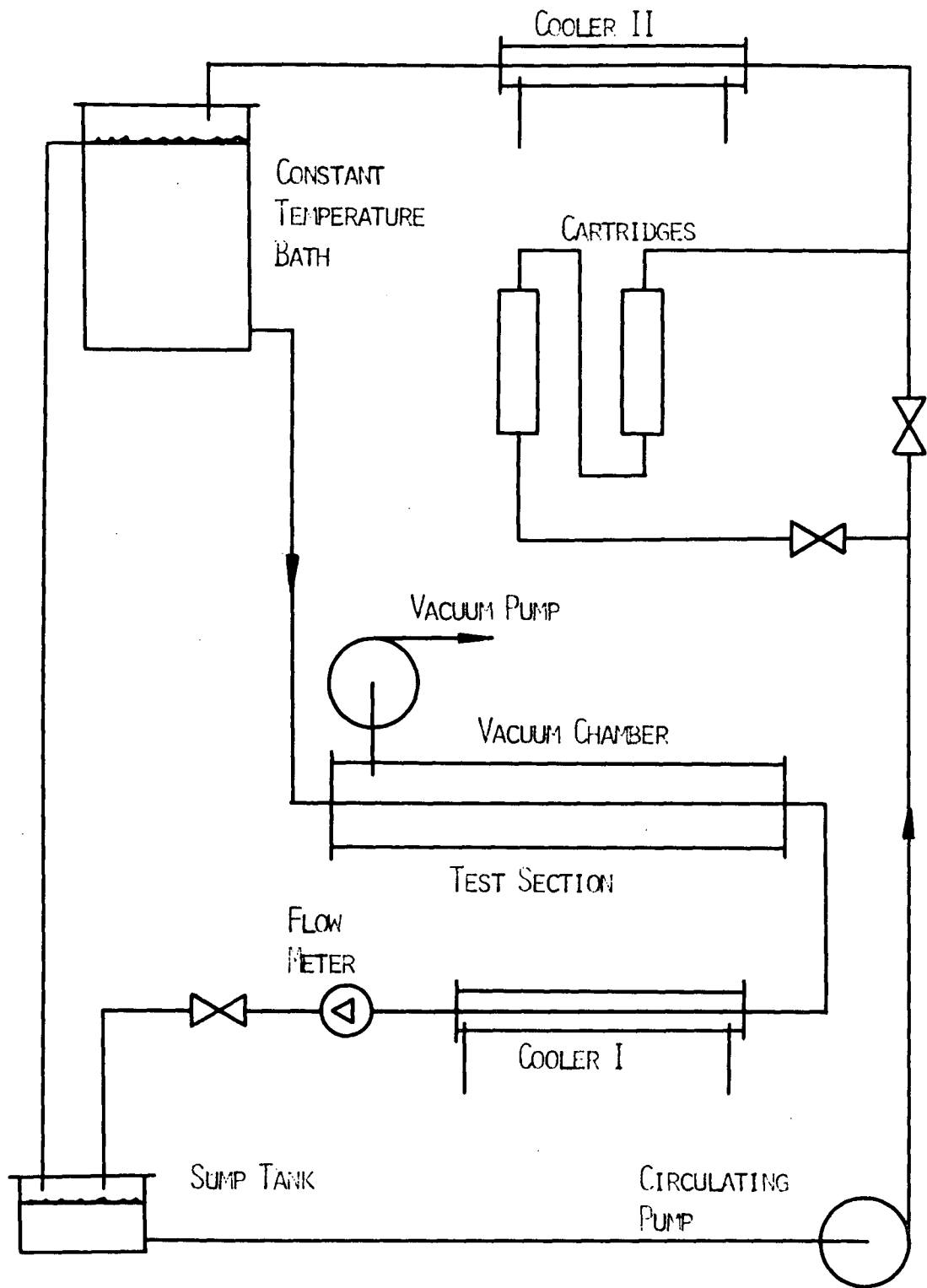


FIGURE 9 SCHEMATIC OF HEAT TRANSFER LOOP

ness Inconel tube. Thermocouples attached to the outer wall enabled determination of the local wall temperature. The test section exit water temperature was measured before being cooled back to approximately room temperature. It then passed through a flowmeter and throttling valve, where the flow rate could be adjusted, and into a sump tank. The exact flow rate was measured by collecting water over a known time interval. A pump circulated the water either through two cartridges in series, or directly into a cooler. One of the cartridges contained a mixed bed ion-exchanger matrix to deionize the water, the other a matrix to remove organic particles from the water. Since the constant temperature bath contained only a heater, inlet temperature was maintained by first cooling the water in a heat exchanger connected to a domestic cold water supply. Fig. 10 shows part of the experimental set up.

Test Section

The test section was an Inconel tube with a 0.25 inch outside diameter and a wall thickness of 10/1000 of an inch. The length of 72 inches gave a length to diameter ratio of about 313. The outside diameter was checked for uniformity over the whole length. An overall inside diameter was also measured, but the uniformity of the wall thickness was not checked. Fig. 11 shows details of the test section.

The test section was desired to have high electrical resistivity, and low thermal conductivity. The former was to obtain a higher resistance and hence lower current by a higher voltage drop, the latter to minimize heat conduction along tube axis. A Nickel Alloy used for resistance

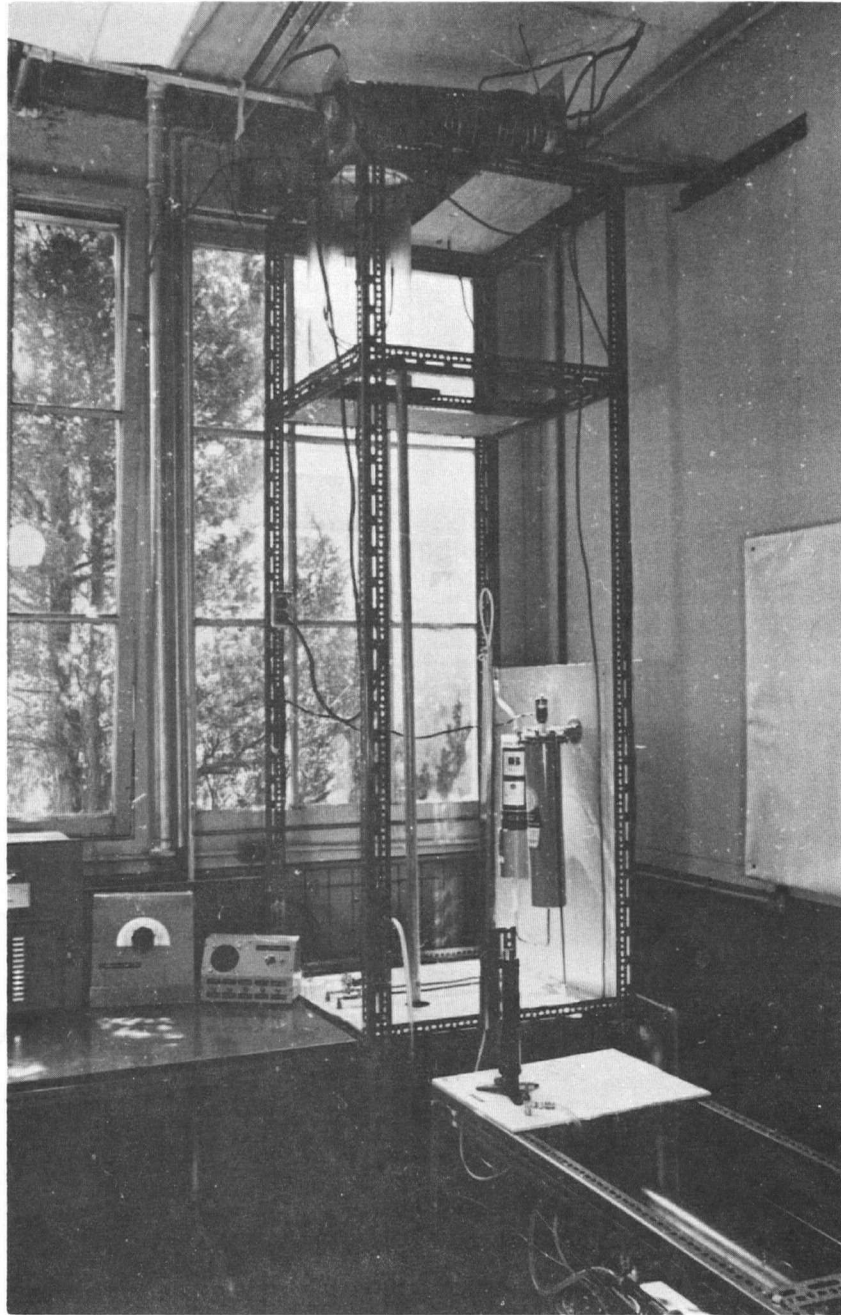
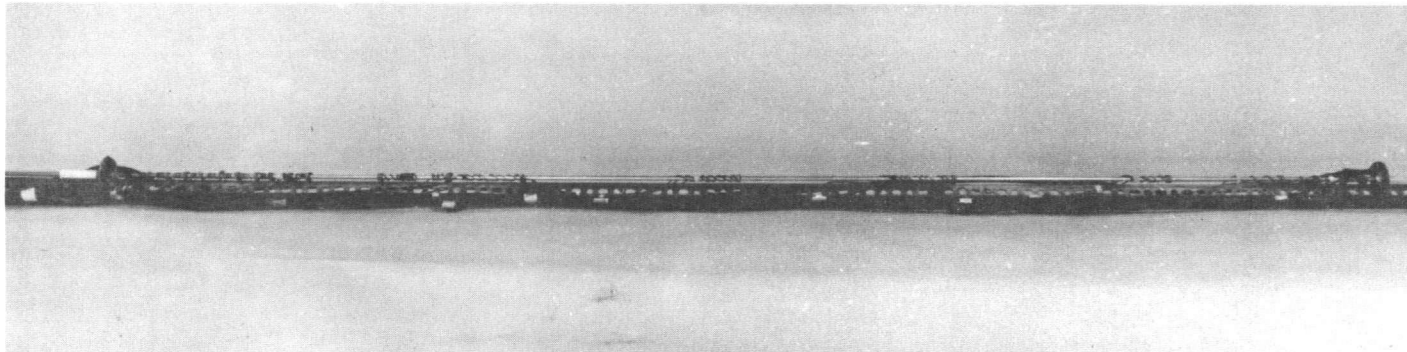
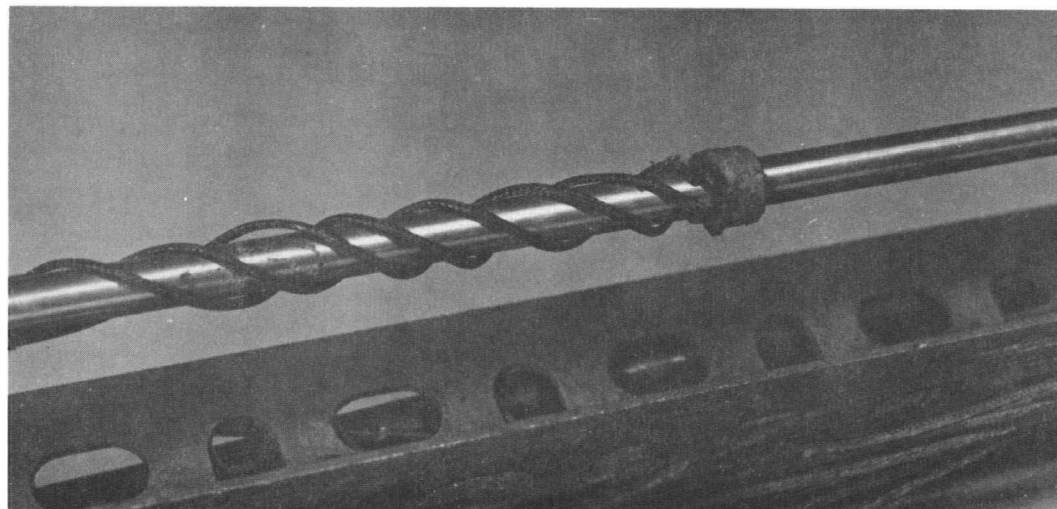


FIGURE 10 PARTIAL VIEW OF EXPERIMENTAL ARRANGEMENT



TEST SECTION



THERMOCOUPLES MOUNTED ON TEST SECTION

FIGURE 11 VIEW OF TEST SECTION

heating satisfies this condition best. A thin tube wall is used since this will reduce thermal conductance and raise the electrical resistance.

An "Inconel X 750" tube was found to be most suitable for this. Thermocouples were mounted on the test tube with small non-conducting clamps in order to maintain good contact between the tube wall and wire junction. To minimize error due to thermocouple conductance the thermocouple wires were wound around the tube a few times.

Due to secondary flow in the test section, higher heat transfer rates are expected from the lower than the upper half of the tube circumference. This gives rise to non-uniform temperature over a circumference at any tube section. In an attempt to take this into account, thermocouples were placed at three points at a tube section as shown in Fig. 12.

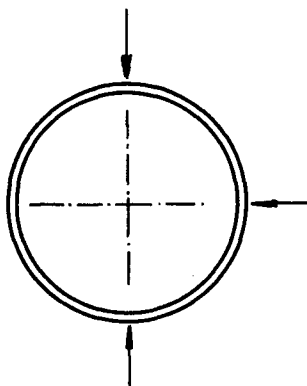


Fig. 12: Thermocouple placing on test section circumference

The axial spacing of thermocouples was 12 inches in the middle part of the tube, and less near each end in order to allow a determination of the entrance length and to detect heat loss due to conductance along power leads and tube wall. The location of the thermocouples is given

in Appendix B. Circular copper flanges were mounted at each end of the test section by a slight press fit. The electrical conductivity was improved by using conductive epoxy silver solder.

The hydrodynamic approach section was thermally insulated from the test tube by a teflon tube of one inch length. The inlet to the hydrodynamic approach had a smooth converging shape, and was also made of teflon.

At the test section exit, a tube of 10 inches in length of the same diameter was used before diverging to a larger diameter. In the larger section, a fine wire mesh was used to provide mixing.

The test section and hydrodynamic approach were placed on a red fibre material with low thermal conductivity.

Test Section Insulation

For the small heat transfer coefficients encountered in laminar flow, the insulation of the test section is very important. Hallman [20] found that use of a vacuum chamber was five times more effective in terms of insulation and attainment of steady state conditions than ordinary insulation material. Therefore this device was applied in this experiment. A ten foot long steel tube of four inches diameter was used as a vacuum chamber, in which the test section and hydrodynamic approach were placed.

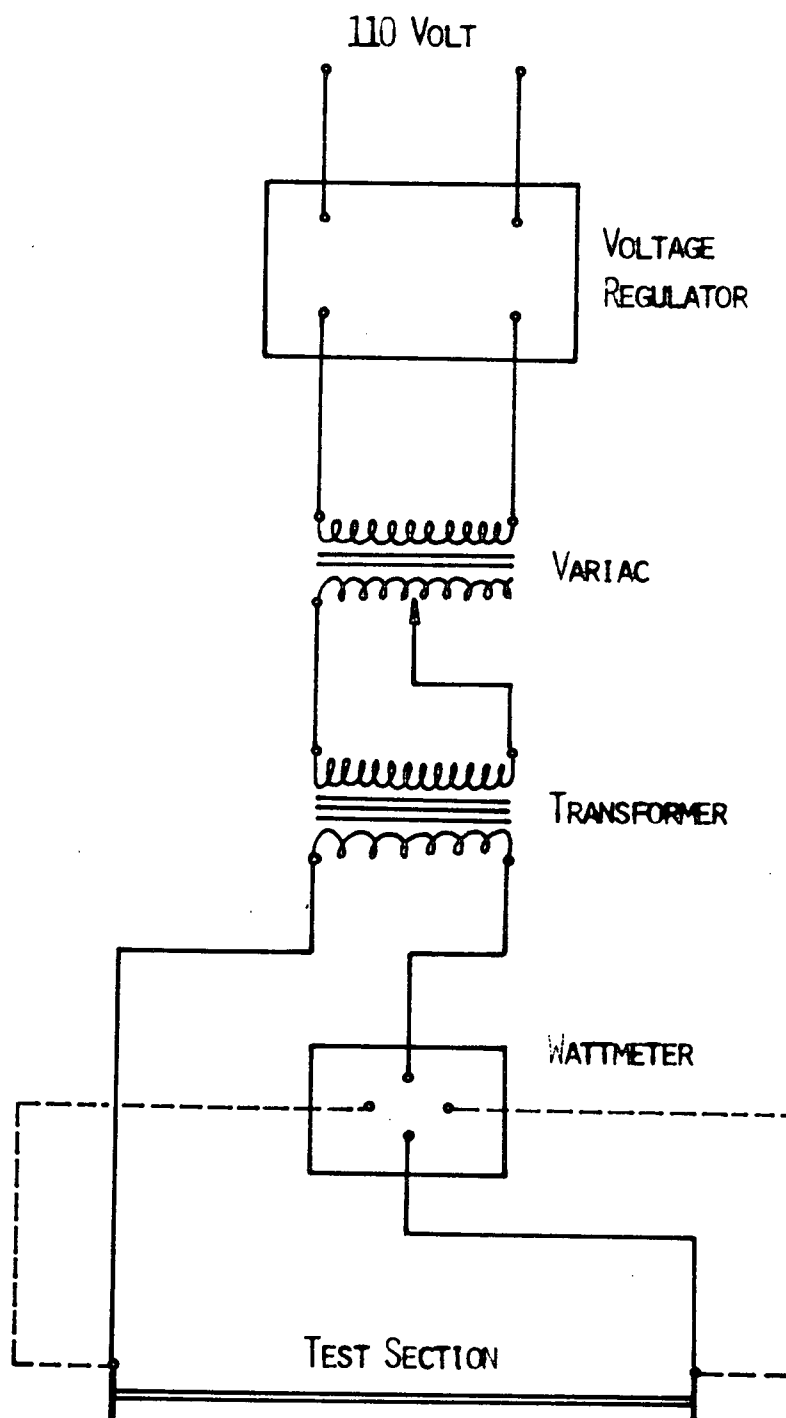


FIGURE 13 SCHEMATIC OF POWER SUPPLY

Power Supply

The test section is resistance heated by a power supply as shown in Fig. 13. Alternating current was employed in order to eliminate voltage pick up across the thermocouple junction. Current passes through a voltage regulator with an accuracy of 1 per cent, and was adjusted by a Variac. A steady step-down transformer gave the required lower voltage. The current then passed through a wattmeter, and to power-leads attached to the test section.

Temperature Measurement

Copper-Constantan thermocouple wire of 30 gauge was used throughout for temperature measurement. There are two groups of thermocouples, as shown in Fig. 14. The first group pertains to thermocouples where less accuracy is required, for example room temperature, and auxiliary temperatures of the flow loop such as temperature in the cooler, flowmeter, etc. These temperatures were measured with a "Honeywell Electronic 15" instrument having an accuracy of 1°F. This instrument has 24 inputs, is self-balancing and does not need a reference junction. The second group of thermocouples measured temperature of the test section wall and the mixing cup temperature. They were selected by a multipole switch, measured either by the Honeywell instrument (for rough readings), or by the K3 Universal potentiometer (for accurate readings). The K3 instrument enables a voltage selection of 0.5 microvolt, and is used with standard cell, galvanometer and reference junction. A melting ice bath was used for a reference junction. Distilled water ice was used for this purpose and was constantly stirred to maintain uniform temperature.

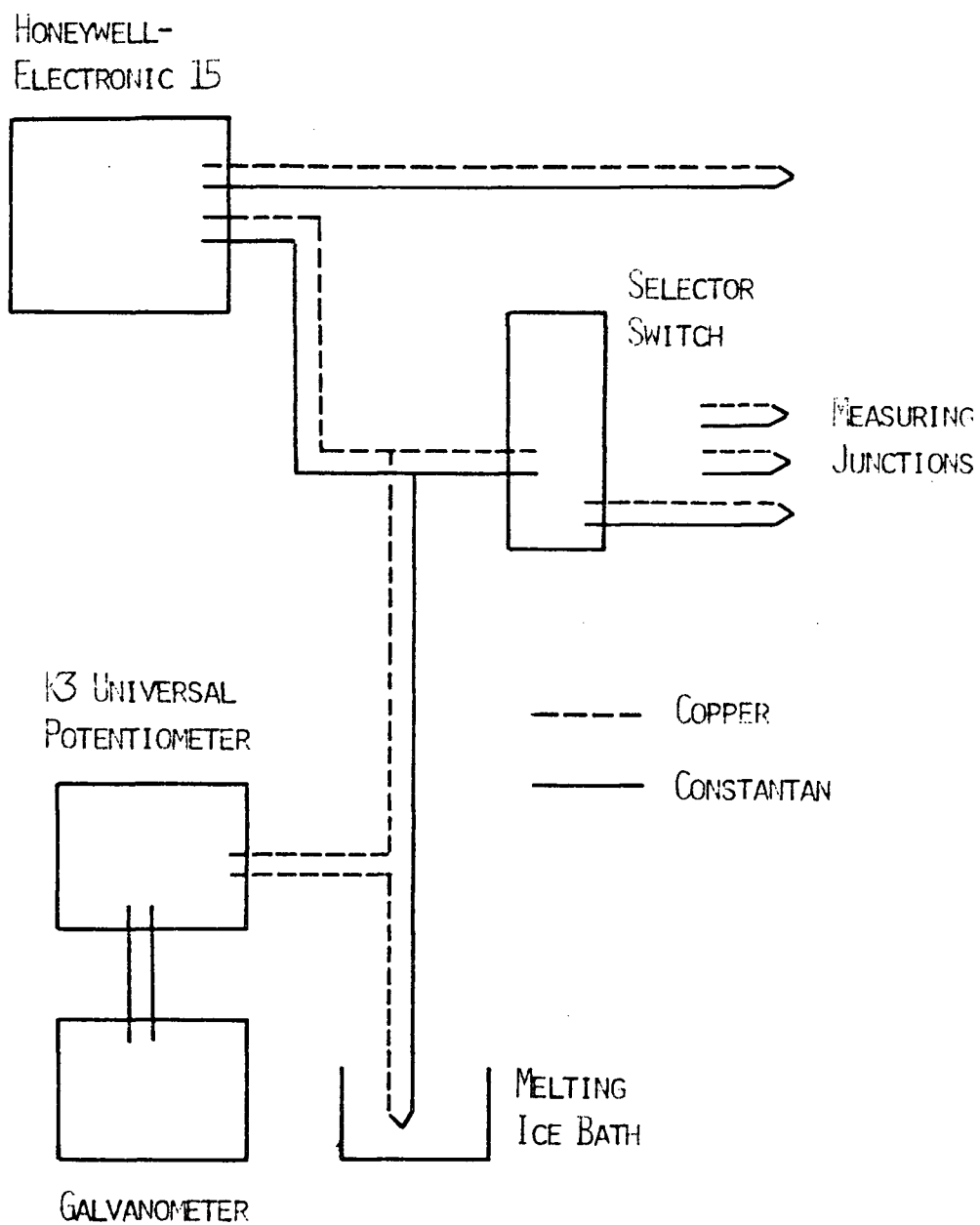


FIGURE 14 THERMOCOUPLE CIRCUIT

EXPERIMENTAL PROCEDURE

Test Procedure

The experimental data were taken in the following manner. A flow rate and a power level were set, and allowed to reach a steady value. When the inlet water temperature attained a steady value, readings were taken of the flow rate, power, water inlet, and outlet temperature, both before and after reading the wall temperature thermocouples.

Thermocouple Calibration Method

The test section and mixing cup thermocouples were calibrated in order to obtain better accuracy in temperature measurements. These thermocouples were calibrated by comparing them with a standard mercury thermometer.

For calibration, all thermocouples were detached from the test section and fastened to the bulb of the mercury thermometer. The hot junctions were then put into a Dewar flask together with the standard thermometer, and water of desired temperature placed in the Dewar flask. Each thermocouple voltage was read simultaneously on the potentiometer and mercury thermometer. This procedure was repeated for four different temperatures (roughly 170, 112, 89, and 55°F) covering the whole region in which thermocouples were used for the test runs. During the calibration the temperature of the ice bath was also measured with a mercury thermometer, and found to vary by 0.1 centigrade.

Calibration Result

The voltage reading of all thermocouples varied not more than five microvolts, which corresponds to 0.25°F . The accuracy of the mercury thermometer was 0.09°F . When the galvanometer was used, one could detect a voltage variation not smaller than 3 to 4 microvolts. Since the thermocouples agreed with each other very closely, they were not treated separately but only one calibration curve was used for all thermocouples.

The data from the calibration procedure were fitted by method of least squares to a second degree polynomial equation of the form

$$T = 32 + C_1 E + C_2 E^2 \quad (16)$$

where T temperature, $^{\circ}\text{F}$

E microvolts

C_1, C_2 constants.

The constants were evaluated, giving the following equation

$$T = 32 + 4.763 \cdot 10^{-2} E - 1.507 \cdot 10^{-6} E^2. \quad (16a)$$

RESULTS AND DISCUSSION

Heat transfer data were obtained for a horizontal circular tube with internal laminar flow. The boundary condition was approximately uniform heat flux over the entire test section. The Reynolds number ranged from 100 to 2000. The Grashof number was varied by applying different rates of heat generation, and the natural convection effect on the forced laminar heat transfer was studied by comparing the high Grashof number runs to runs at lower Grashof number at approximately the same Reynolds number. Since water was used as the heat transfer medium the Prandtl number could be changed only by using a different temperature range.

The flow was considered laminar when no wall temperature fluctuations were present. While taking temperature readings, one could observe when the flow was changing from steady laminar to random eddying flow.

The limit of laminar flow is dependent on Reynolds number and Grashof number. It was found that at a certain Reynolds number the transition flow was present if heat flux was high enough, that is, high Grashof number. A smaller Reynolds number stabilized the flow. It was not the purpose of the present work to investigate the limits of laminar flow. These observations were merely to omit data in the transition or turbulent flow region.

Entrance Length and Circumferential Temperature Variation

Similar to the development of a laminar velocity profile, the temperature profile needs a certain axial distance to become fully-developed. The entrance region is determined from measurement of the axial wall temperature gradient. Consider the fluid temperature profile as shown in Fig. 15. At the entrance to the heated section the temperature is uniform. As the fluid moves downstream, heat is removed from the wall and the temperature difference between fluid and the wall is increased. In the tube center there is a core of fluid which is still at the same temperature as in the unheated section. As the fluid moves further downstream the core diminishes and finally disappears. This is the point when the temperature profile is considered fully-developed. For pure forced convection and laminar flow, the entrance length will be different than the present case under investigation.

Fig. 16 shows temperature profiles for run number 42. Between $X/D = 100$ and 300 the Reynolds number increases from 669 to 742, and the Grashof number from 1269 to 1541. The flow can be considered fully-developed approximately from the point $X/D = 75$. At $X/D = 104$ the difference between bottom and top wall temperature is 2.6°F , while further downstream the difference between bottom and top wall temperature increases to become a maximum of 5.9°F at about $X/D = 200$, and then decreases slightly towards the test section end.

It may be noted from Fig. 16 that in the entrance region the wall temperature gradient is high at the tube inlet, and decreases slowly in

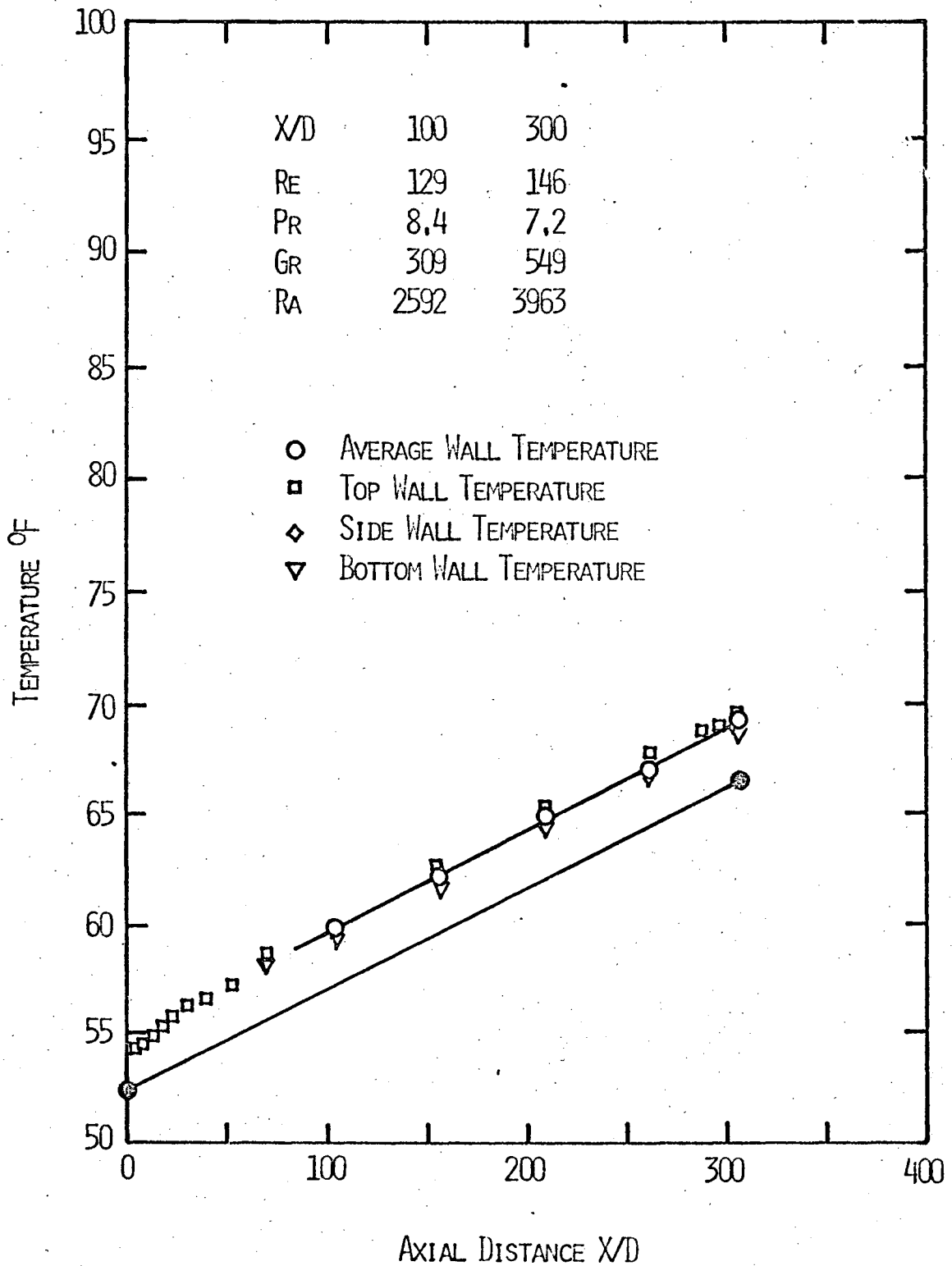


FIGURE 15 REPRESENTATIVE TEMPERATURE PROFILE
RUN NUMBER 3

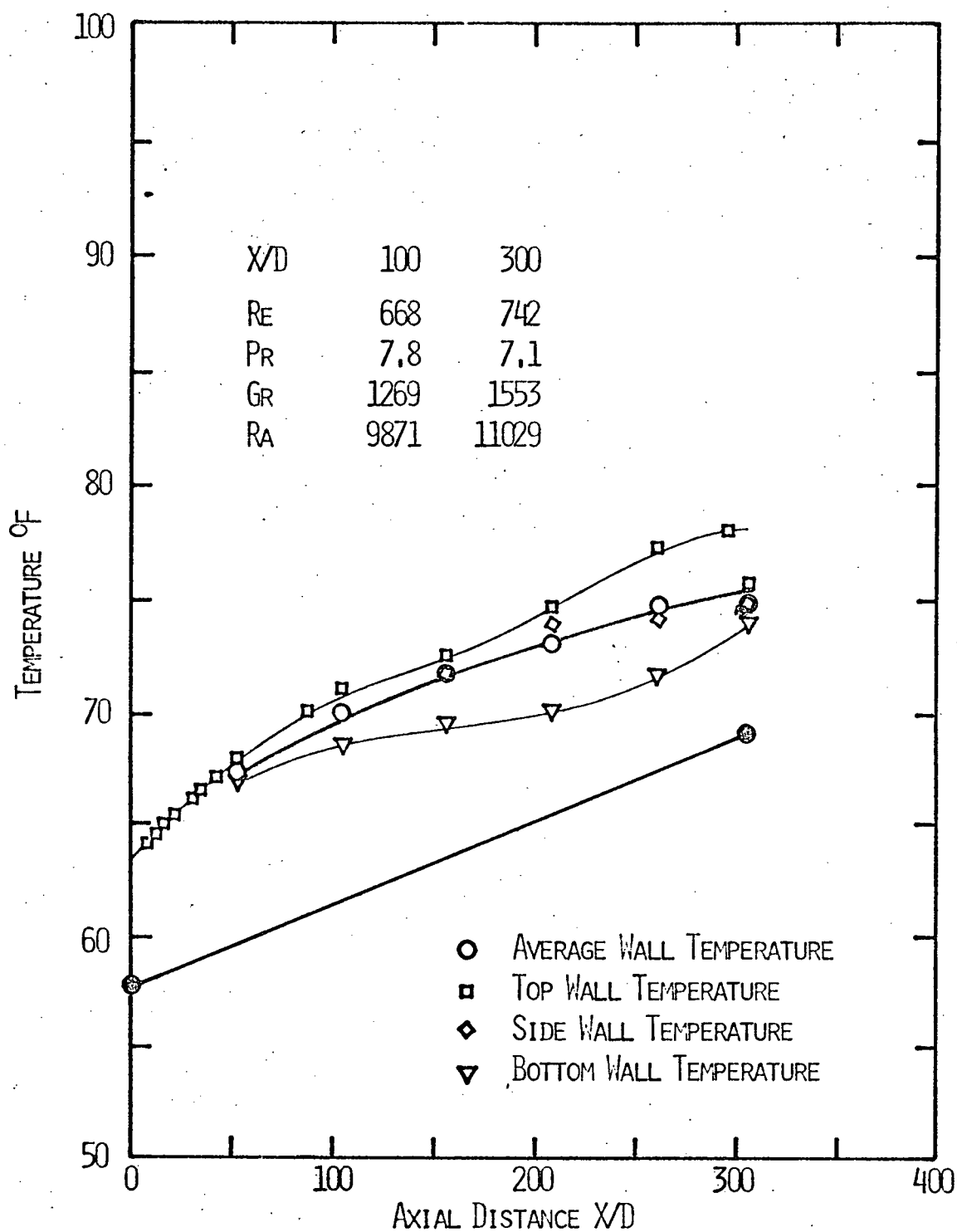


FIGURE 16 REPRESENTATIVE TEMPERATURE PROFILE
RUN NUMBER 42

the axial direction. At about 100 diameters downstream it becomes almost constant.

Axial Temperature Profiles

Fig. 17 shows the tube wall temperature and the fluid bulk temperature for run number 1. Between $X/D = 100$ and 300 the Reynolds number varies from 366 to 408, and the Grashof number from 703 to 965. Downstream of $X/D = 100$ the average wall temperature remains constant. The difference between fluid bulk and mean wall temperature is 5.7°F at $X/D = 100$, and decreases slightly to 4.6°F at the test section exit. The difference between bottom and top wall temperature is approximately 1.5°F , or nearly 30 per cent of the difference between mean wall and fluid bulk temperature.

Fig. 18 shows the temperature profiles for run number 43. The Reynolds number is 331 at the inlet to the heated section. This test run was performed with higher heat flux, giving a Grashof number of the order of 2000. The gradient of the average wall temperature decreases until approximately $X/D = 60$; from here on downstream it remains constant. Average wall and fluid bulk temperature profiles are not parallel. The difference between fluid bulk and mean wall temperature is 8.8°F at $X/D = 100$, and decreases to 6.7°F at $X/D = 300$.

One should not expect the fluid bulk temperature gradient and the mean wall temperature gradient to be exactly the same. With change of the fluid bulk temperature the properties of water change, and this causes a change in the dimensionless numbers such as Reynolds, Grashof, and

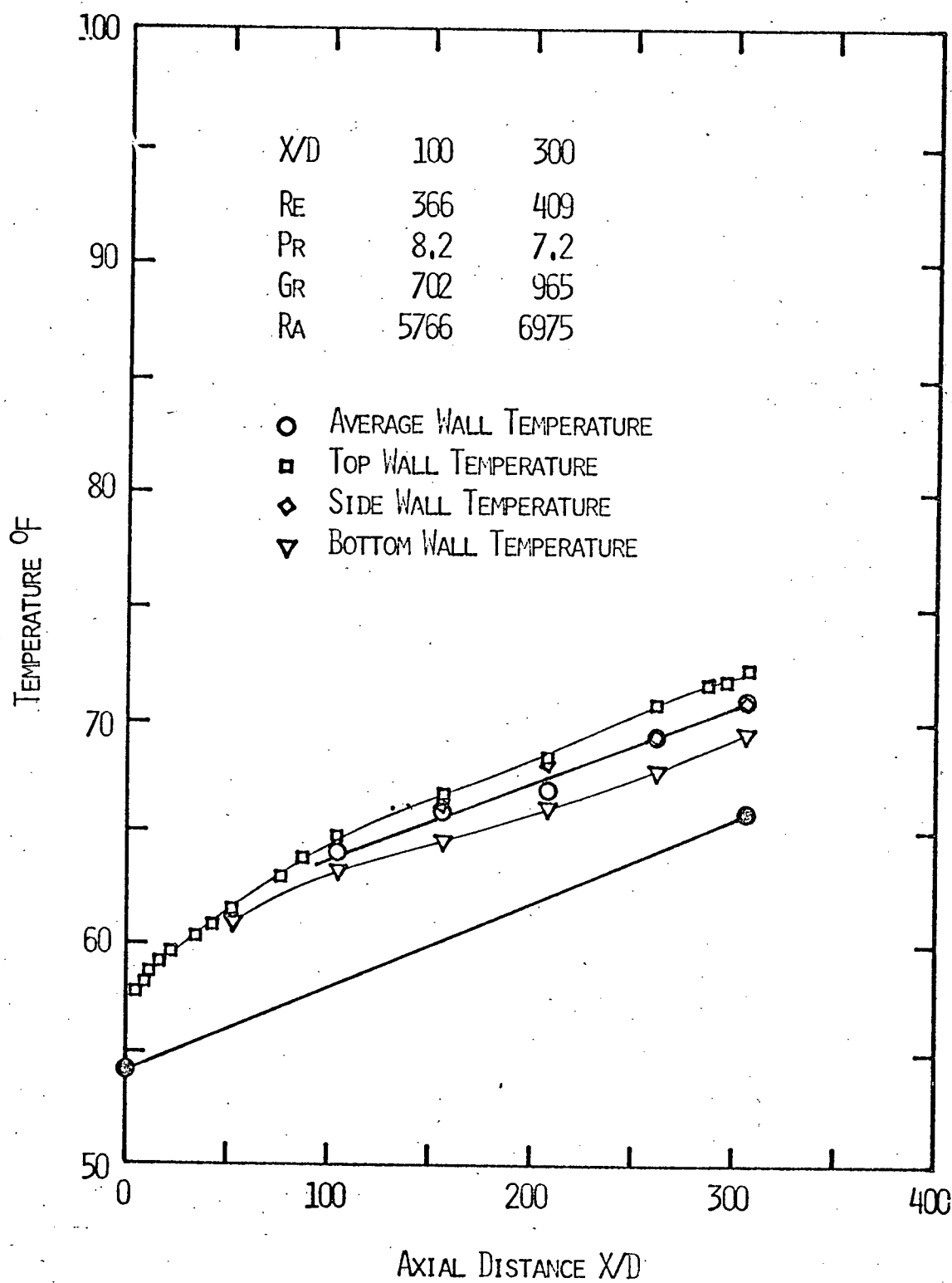


FIGURE 17 REPRESENTATIVE TEMPERATURE PROFILE
RUN NUMBER 1

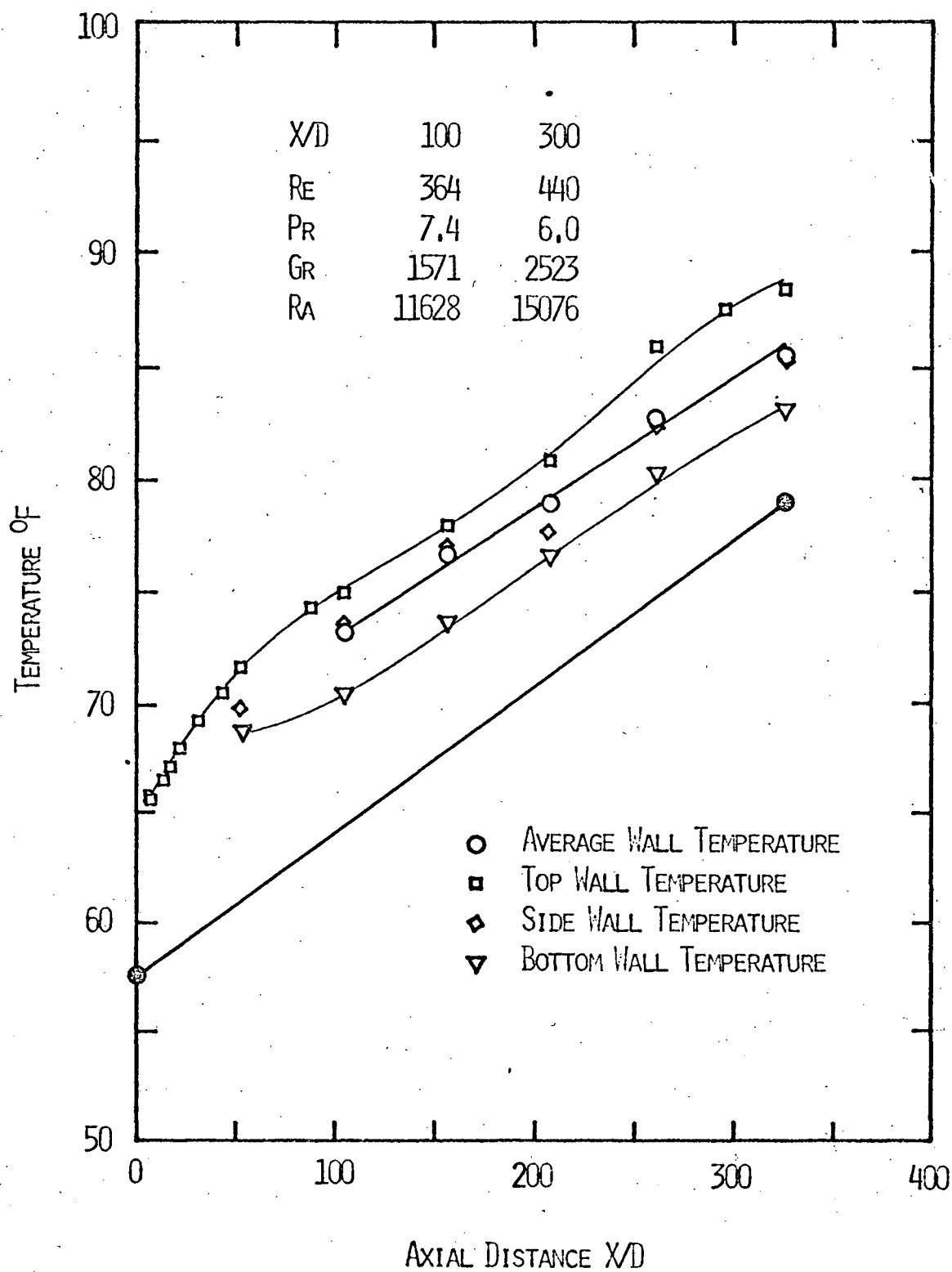


FIGURE 18 REPRESENTATIVE TEMPERATURE PROFILE
 RUN NUMBER 43

Prandtl numbers. The heat flux is the same over the entire test section, but a change in the free convection effect influences the heat transfer rate, therefore the temperature difference will change. In the test run considered, (Fig. 18), the Reynolds number increases from 364 at $X/D = 104$, to 440 at $X/D = 306$. In the same section the Prandtl number changes from 7.4 to 6.0, and the Grashof number increases from 1571 to 2523.

Fig. 19 shows the temperature profile of run number 37, which covered Reynolds numbers in the region of 1150 to 1300. The Grashof number varied approximately from 2300 to 3600. The temperature difference in the entrance region increased rapidly, then decreased slightly towards the test section exit.

Fig. 20 shows the temperature profile for a test run with high flow rate and heat flux. The Reynolds number varies from 1374 to 1600, and the Grashof number from 6000 to 9600. The temperature difference between mean wall and fluid bulk is nearly 20°F at $X/D = 200$. A large circumferential temperature difference is produced due to the high heat flux.

When Figs. 17, 18, 19, and 20 are compared with each other, one notices a consistent dropping of the average wall temperature near the tube exit. This dropping is more pronounced in higher Grashof number runs.

Local Nusselt Number

Fig. 21 shows the Nusselt number profile for a run with Reynolds numbers in the order of 130, and with Grashof numbers ranging from 117 to 500. The curve closely resembles the prediction for pure forced convec-

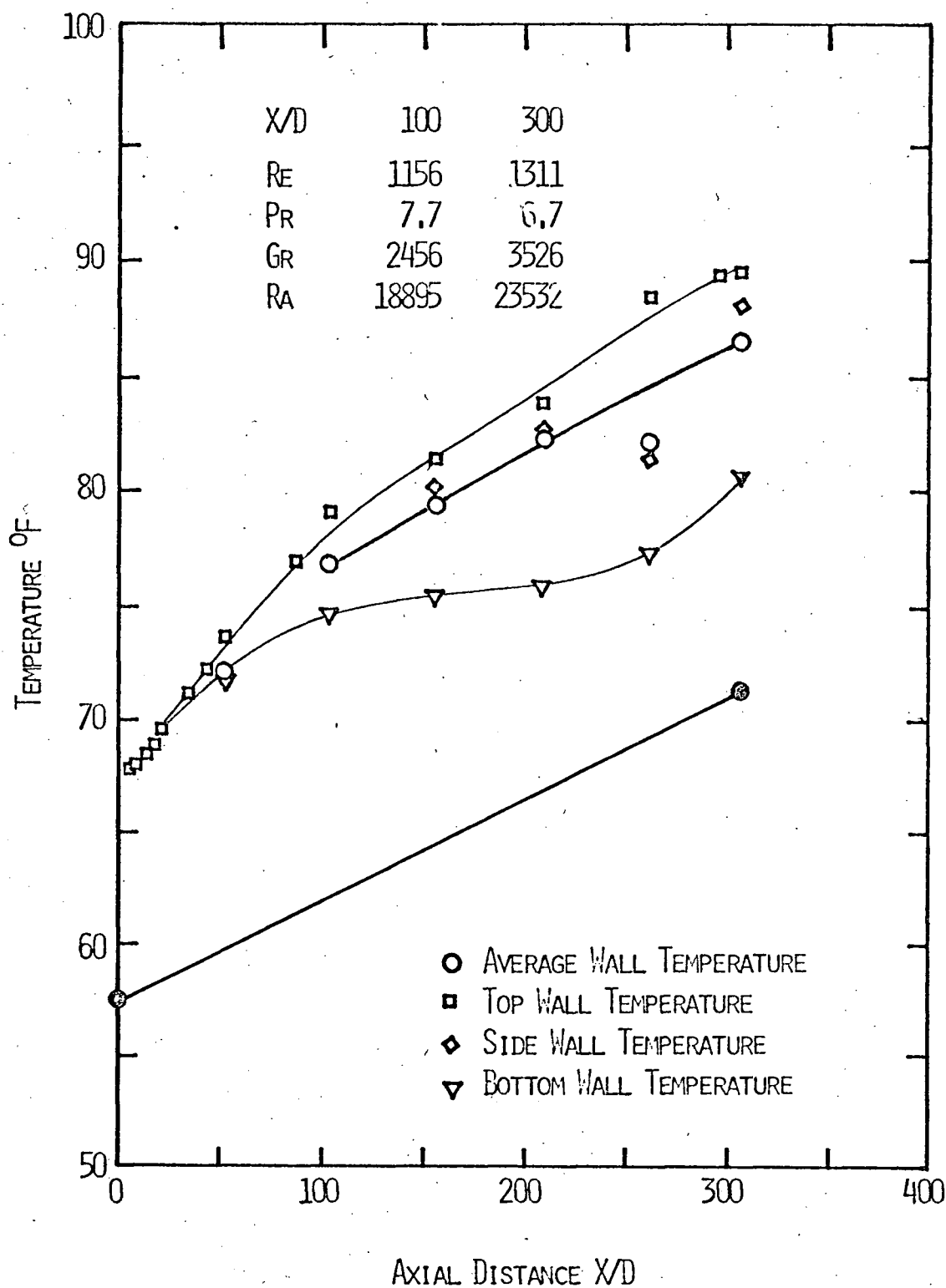


FIGURE 19 REPRESENTATIVE TEMPERATURE PROFILE
 , RUN NUMBER 37

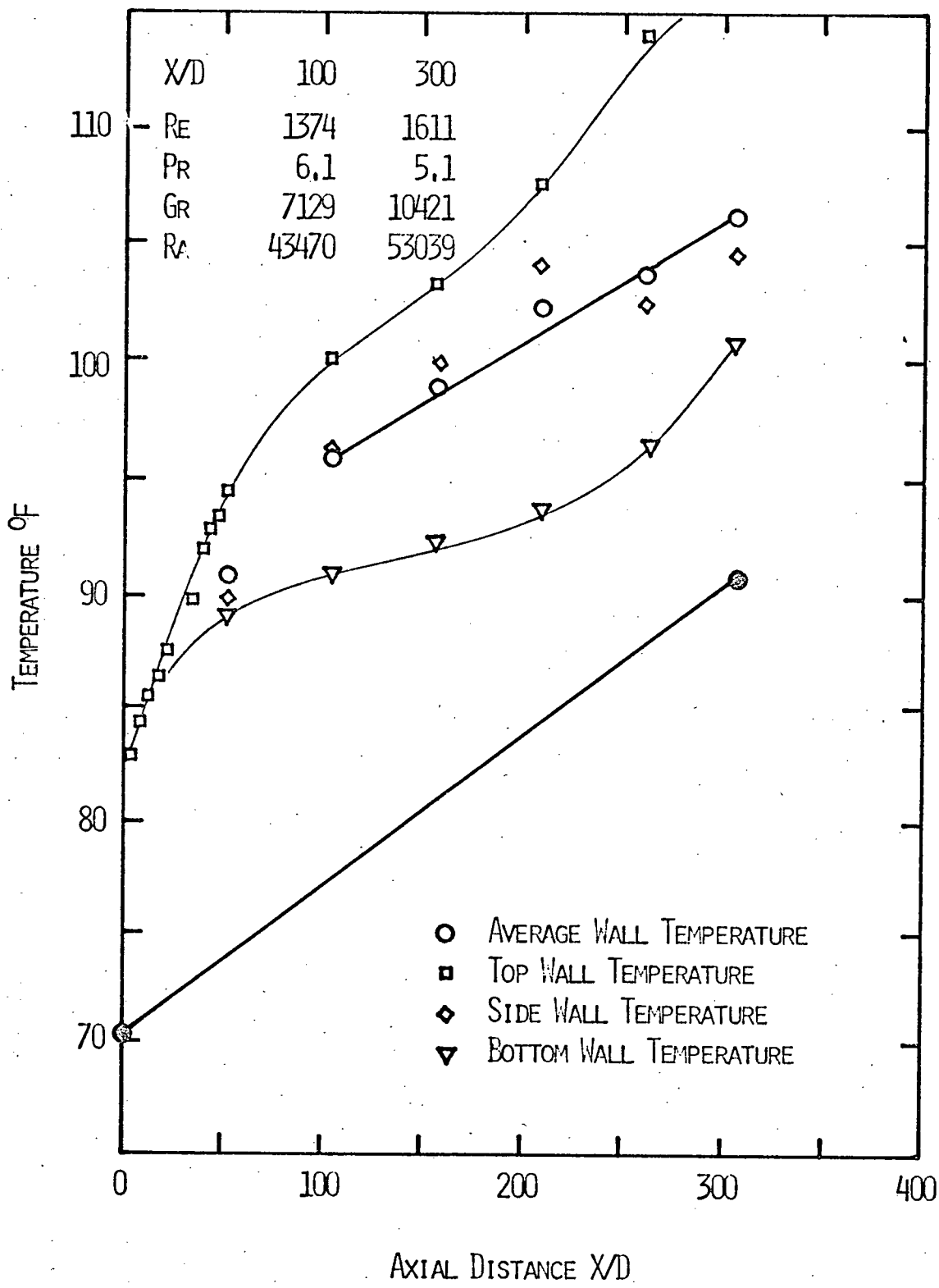


FIGURE 20 REPRESENTATIVE TEMPERATURE PROFILE
 RUN NUMBER 27

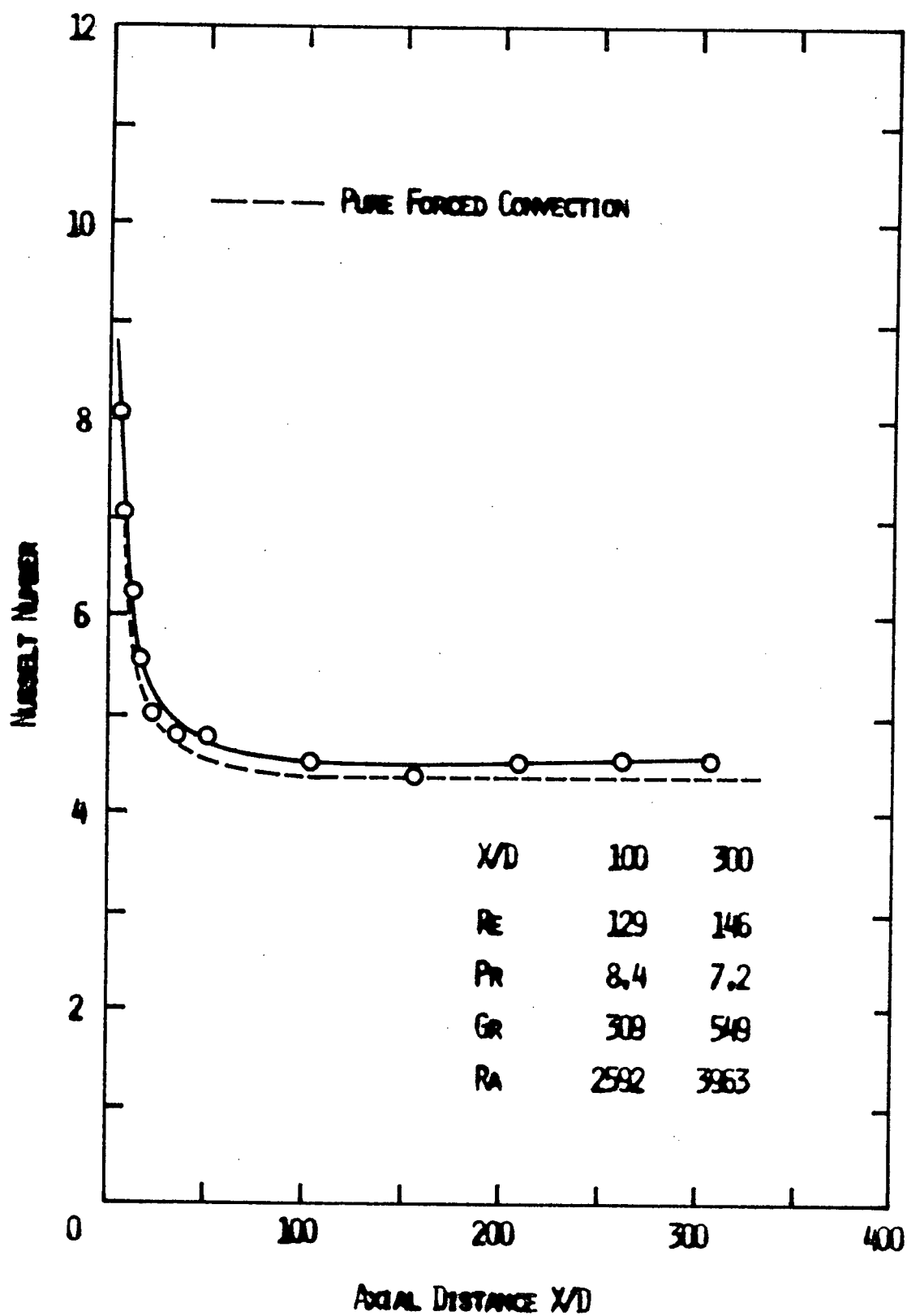


FIGURE 21 REPRESENTATIVE NUSSULT NUMBER PROFILE
RUN NUMBER 3

tion (dashed line). The Nusselt numbers are slightly higher than 4.36, the value predicted for pure forced convection.

Fig. 22 represents a Nusselt number profile with the Reynolds number in the order of 1100 to 1300 and the Grashof number of about 20,000. Due to the high Reynolds number, the temperature profile requires a larger distance to become established inspite of the very high Grashof number.

Fig. 23 shows the plot of Nusselt number versus axial tube distance for run number 1. Reynolds numbers are of the order of 370, while Grashof numbers vary from 700 to 970. At the beginning of the heated section there is a high heat transfer rate. The Nusselt number then decreases rapidly as the temperature profile develops, and at $X/D = 100$ the curve reaches its minimum. This point coincides with the temperature profile becoming fully-developed (Fig. 23). From this point onwards the Nusselt number increases with approximately constant slope.

Fig. 24 represents the Nusselt number variation for run 43. Reynolds and Grashof numbers are in the order of 370 and 1600 respectively. At the tube inlet the Nusselt number is approximately 9. It decreases to a minimum at $X/D = 60$, and then increases at a constant rate.

Comparing run number 1 and 43 (replotted in Fig. 25), we notice that in the second case flow development is achieved in shorter distance, that is a higher Grashof number seems to accelerate flow development. At $X/D = 104$ it appears that the Reynolds numbers are the same. It is interesting to study the effect of Grashof number on Nusselt number at this point. It appears that the higher Grashof number causes an increase in the

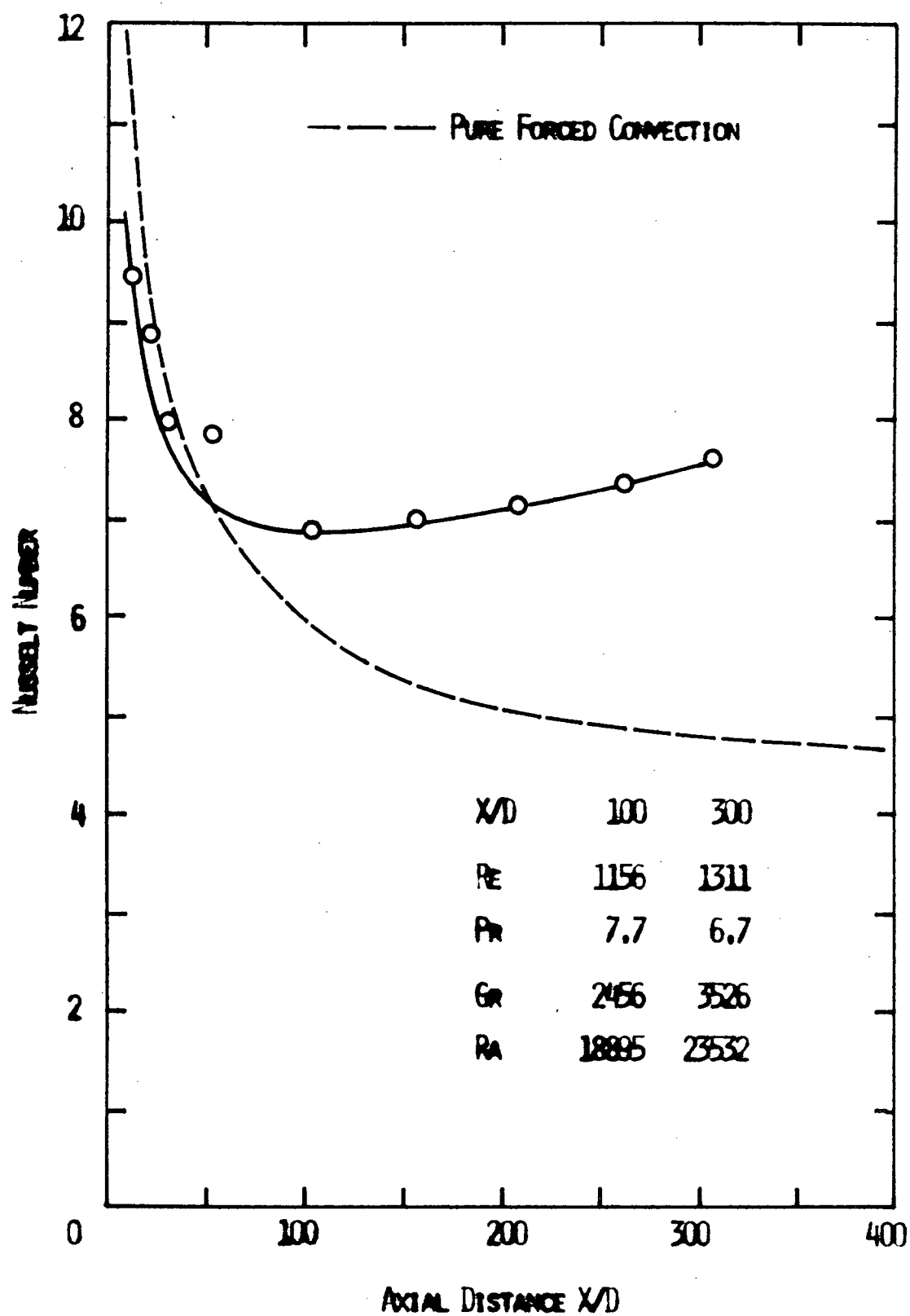


FIGURE 22 REPRESENTATIVE NUSSELT NUMBER PROFILE
RUN NUMBER 37

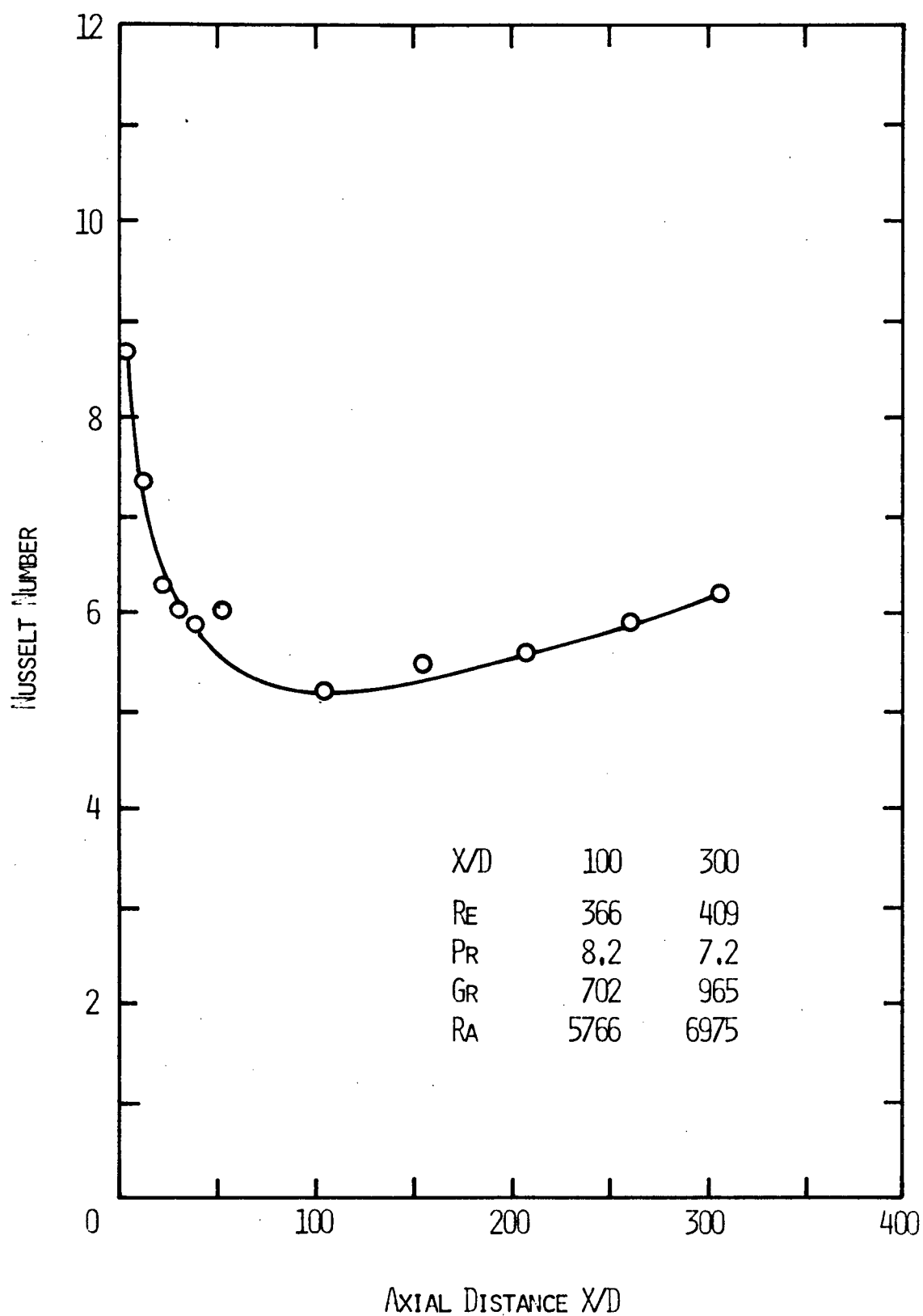


FIGURE 23 REPRESENTATIVE NUSSLETT NUMBER PROFILE
RUN NUMBER 1

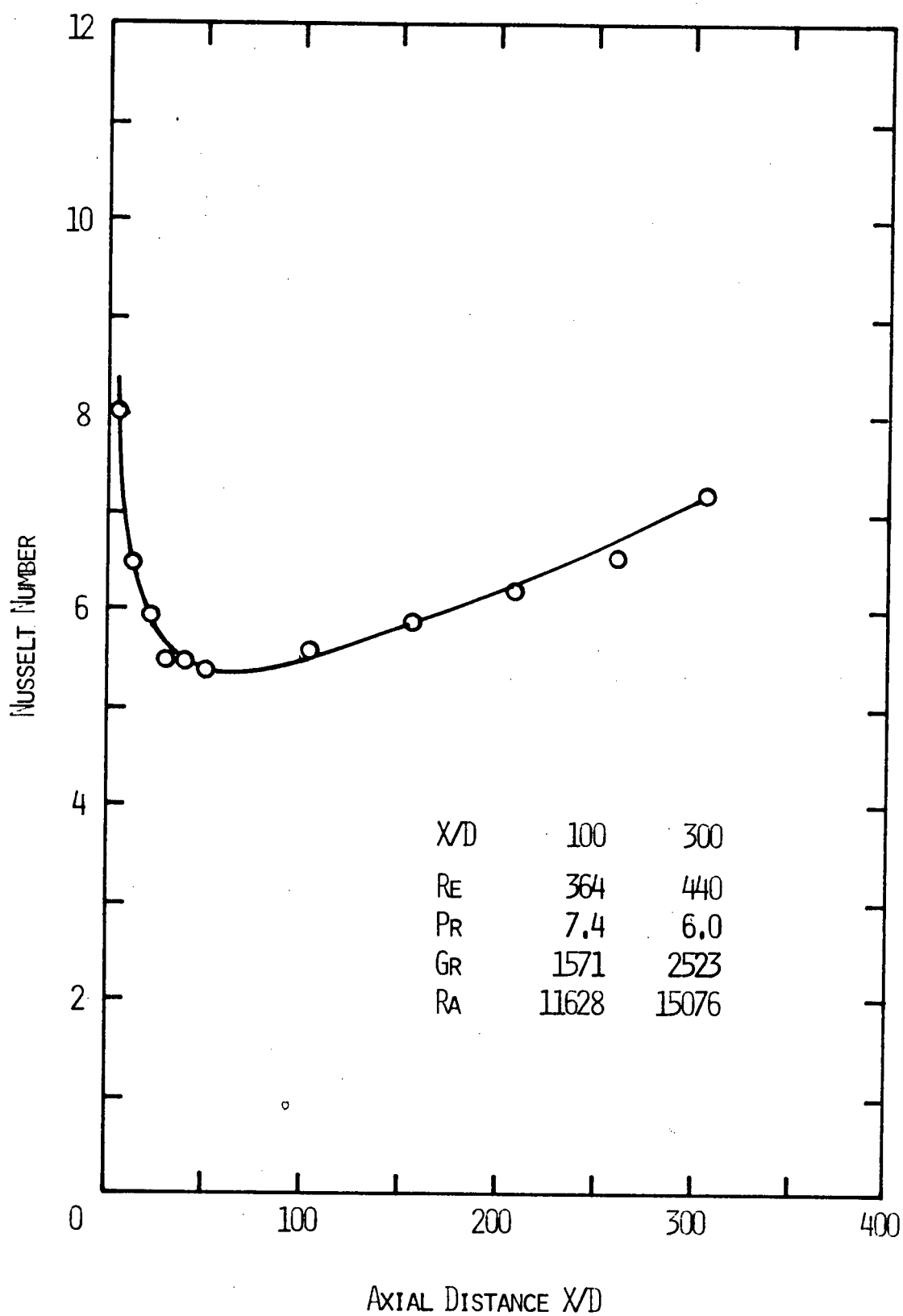


FIGURE 20 REPRESENTATIVE NUSSELT NUMBER PROFILE
RUN NUMBER 43

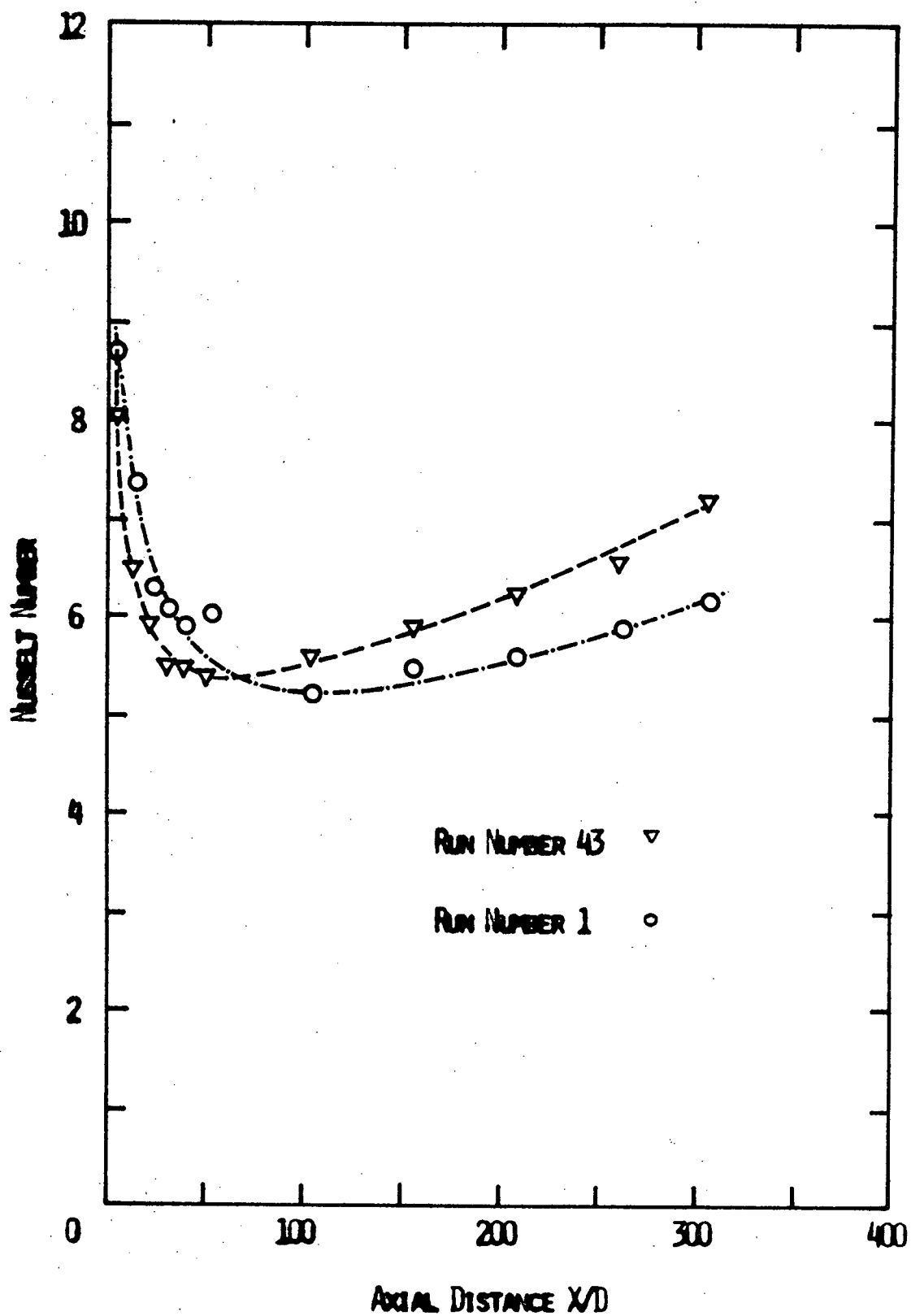


FIGURE 25 REPRESENTATIVE NUSSELT NUMBER PROFILES
RUN NUMBERS 1 AND 43

Nusselt number from 5.2 in run 1 to 5.6 in run 43. Furthermore the Nusselt number increases at a greater rate.

Heat Transfer Correlation

Correlation of overall heat transfer coefficients for the entire test section length with combined free and forced convection under uniform heat flux is complicated by the fact that the free convection effects do not start at the tube inlet, but require a starting length to be established. For uniform wall temperature, both the ratio D/L and L/D were used [8] to give fair correlation. For uniform wall heat flux it appears that there is a pronounced development region to establish the secondary flow, and a region of thermally developed flow where the heat transfer coefficients are dependent only on the parameters Gr , Re , Pr .

Several correlations were tested on the data. The expression

$$Nu = \frac{48}{11} + 0.047 Pr^{1/3} (Re Ra)^{1/5} \quad (17)$$

appears to correlate 53 per cent of the data (plotted in Fig. 26) in the fully-developed region to within ± 10 per cent. Another slightly more accurate expression which correlates 68 per cent of the data to within ± 10 per cent but does not satisfy the pure forced convection case is

$$Nu = 2.41 + 0.082 Pr^{1/3} (Re Ra)^{1/5} \quad (18)$$

This data is plotted in Fig. 27. A point of caution might be added here. The above correlations do not apply to fluids of Prandtl numbers higher than 10, where the additional factor of variation of viscosity with

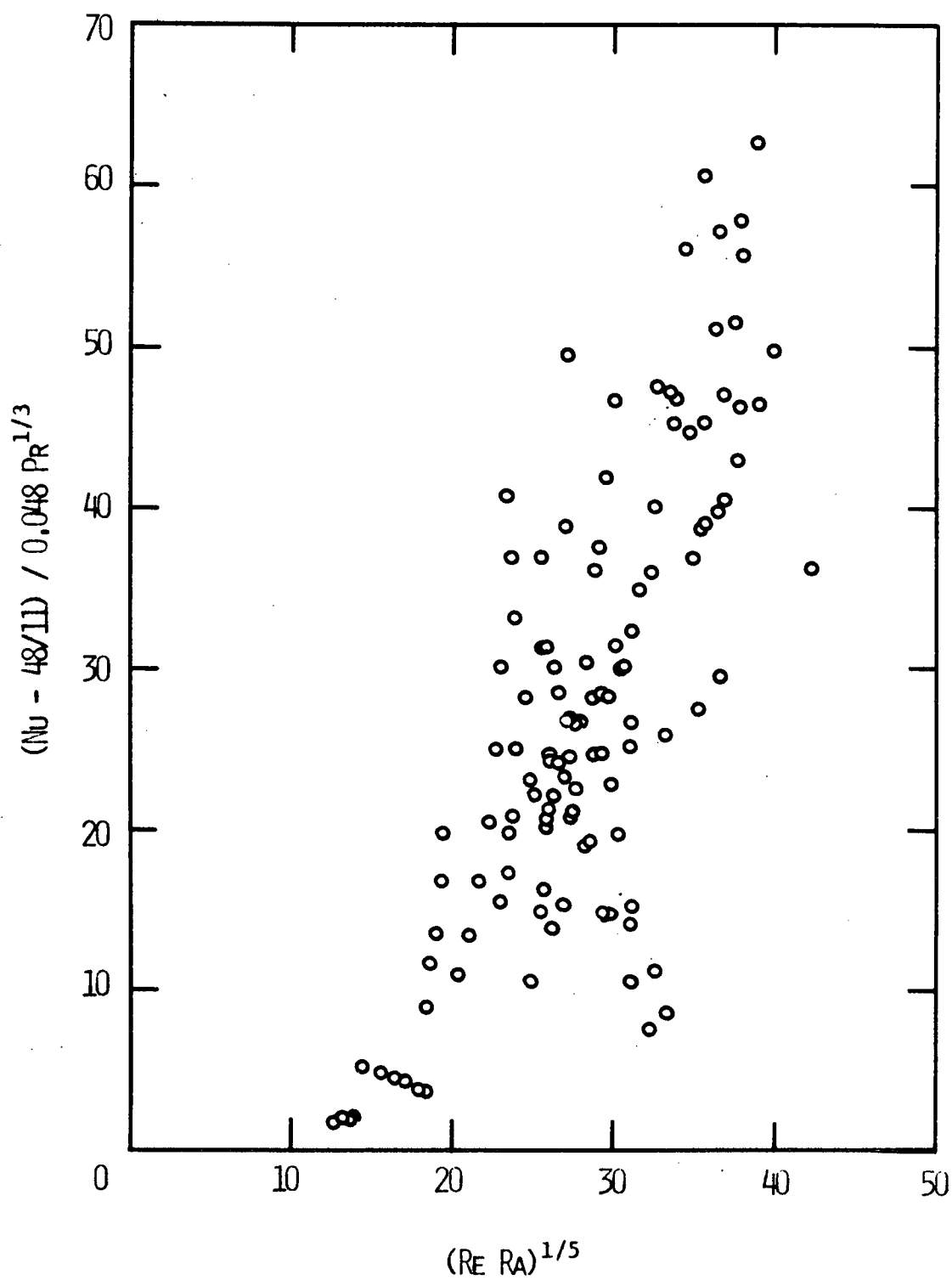


FIGURE 26 CORRELATION OF NUSSELT NUMBER,
EQUATION 17

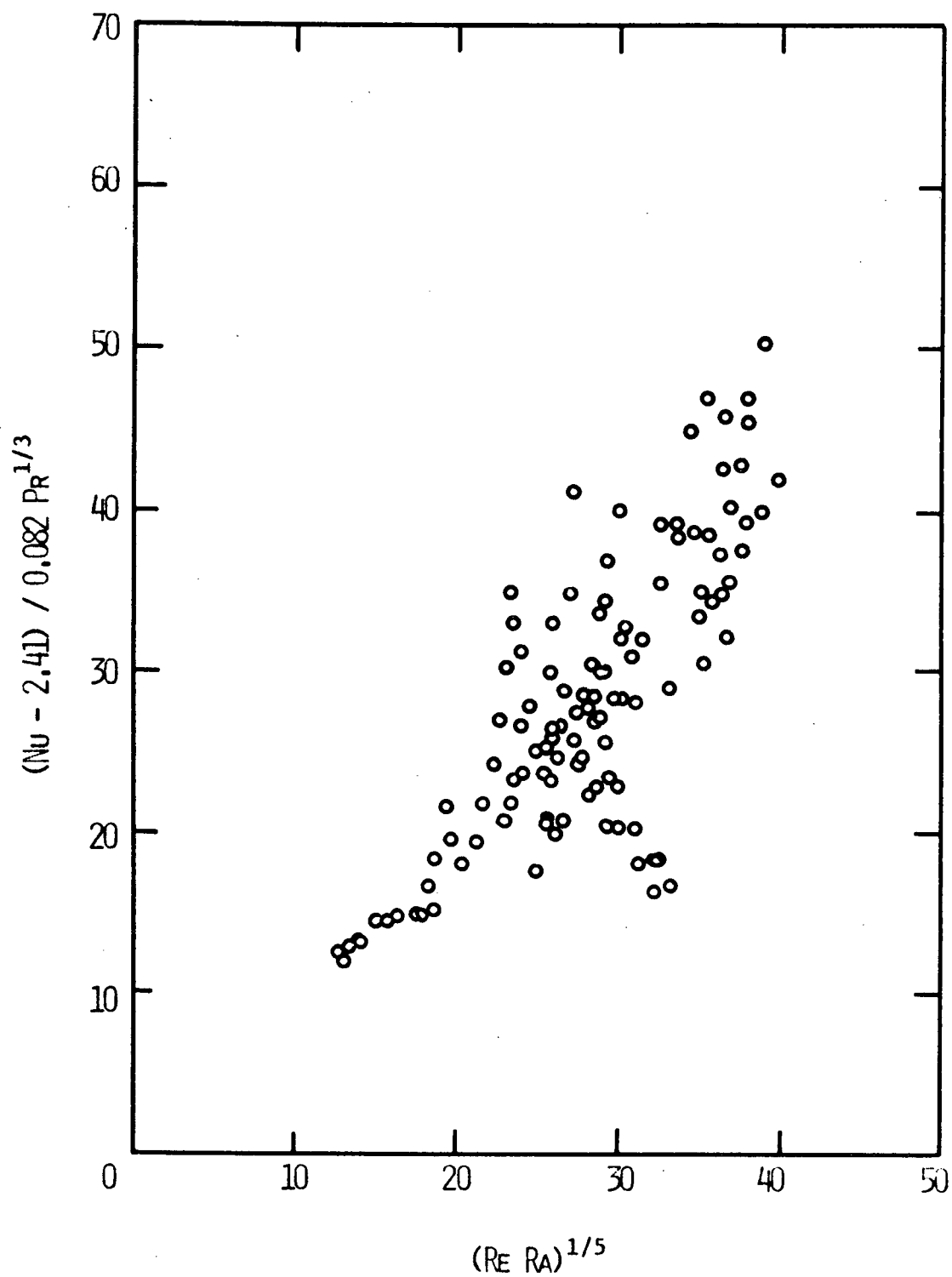


FIGURE 27 CORRELATION OF NUSSELT NUMBER,
EQUATION 18

temperature is dominant also. The expressions (17) and (18) should be considered as very tentative.

Further studies using various other fluids, tube sizes, and lengths are required in order to verify these correlations, and perhaps shed further light on the basic nature of this problem.

CONCLUSION

From this investigation experimental data was obtained for combined free and forced convection laminar heat transfer for water flowing through a circular horizontal tube with uniform heat flux. Results show that at low values of Grashof number the Nusselt number is in good agreement with theoretical prediction for pure forced convection. High Grashof numbers reveal that the free convection effect will create substantial increase in Nusselt number. Two tentative correlations for the Nusselt number for fully-developed flow are given in equation (17) and (18) as a function of Re , Ra and Pr .

REFERENCES

1. A.P. Colburn, "A Method of Correlating Forced Convection Heat Transfer Data and a Comparison with Fluid Friction," Trans. AIChE, vol. 29, 1933, pp. 174 - 210.
2. E.N. Sieder and G.E. Tate, "Heat Transfer and Pressure Drop of Liquids in Tubes," Ind. Eng. Chem., vol. 28, 1936, pp. 1429 - 1435.
3. D.G. Kern and D.F. Othmer, "Effect of Free Convection on Viscous Heat Transfer in Horizontal Tubes," Trans. AIChE, vol. 39, 1943, pp. 517 - 555.
4. R.C. Martinelli, C.J. Southwell, G. Alves, H.L. Craig, E.B. Weinberg, N.F. Lansing, and L.M.K. Boelter, "Heat Transfer and Pressure Drop for a Fluid Flowing in the Viscous Region through a Vertical Pipe," Heat Transfer Data, Part I, Trans. AIChE, vol. 38, 1942, pp. 493 - 530.
5. O.C. Eubank and M.S. Proctor, "Effect of Natural Convection on Heat Transfer with Laminar Flow in Tubes," M.S. Thesis in Chemical Engineering, Massachusetts Institute of Technology, Cambridge, 1951.
6. W.H. McAdams, "Heat Transmission," Third Edition McGraw Hill Book Co., Inc., New York, 1954, p. 235.
7. T.W. Jackson, J.M. Spurlock, and K.R. Purdy, "Combined Free and Forced Convection in a Constant Temperature Horizontal Tube," Journal AIChE, vol. 7, 1961, pp. 38 - 41.

8. D.R. Oliver, "The Effect of Natural Convection on Viscous Flow Heat Transfer in Horizontal Tubes," Chemical Engineering Science, vol. 17, 1962, pp. 335 - 350.
9. A.R. Brown and M.A. Thomas, "Combined Free and Forced Convection Heat Transfer for Laminar Flow in Horizontal Tubes," Journal Mechanical Engineering Science, vol. 7, 1965, pp. 440 - 448.
10. J.J. Martin and M.D. Carmichael, "Combined Forced and Free Convective Heat Transfer in a Horizontal Pipe," ASME, Paper No. 55-A-30, 1955.
11. B.R. Morton, "Laminar Convection in Uniformly Heated Horizontal Pipes at Low Rayleigh Numbers," Quarterly Journal of Mechanics and Applied Mathematics, vol. 12, no. 4, 1959, pp. 410 - 420.
12. M. Iqbal and J.W. Stachiewicz, "Influence of Tube Orientation on Combined Free and Forced Laminar Convection Heat Transfer," Journal of Heat Transfer, Trans. ASME, Series C, 1966, pp. 109 - 116.
13. E. Del Casal and N.N. Gill, "A Note on Natural Convection Effects in Fully Developed Flow," Journal AIChE, vol. 8, 1962, pp. 570 - 574.
14. A.J. Ede, "The Heat Transfer Coefficient for Flow in a Pipe," International Journal of Heat and Mass Transfer, vol. 4, 1961, pp. 105 - 110.
15. S.T. McComas and E.R.G. Eckert, "Combined Free and Forced Convection in a Horizontal Circular Tube," Journal of Heat Transfer, Trans. ASME, Series C, 1966, pp. 147 - 153.

16. Y. Mori, K. Futagami, S. Tokida, and M. Nakamura, "Forced Convective Heat Transfer in Uniformly Heated Horizontal Tubes," International Journal of Heat and Mass Transfer, vol. 9, 1966, pp. 453 - 463.
17. Y. Mori and K. Futagami, "Forced Convective Heat Transfer in Uniformly Heated Horizontal Tubes," International Journal of Heat and Mass Transfer, vol. 10, 1967, pp. 1801 - 1813.
18. R.L. Shannon and C.A. Depew, "Combined Free and Forced Laminar Convection in a Horizontal Tube with Uniform Heat Flux," ASME Paper No. 67-HT-52, 1967.
19. R. Siegel, E.M. Sparrow, and T.M. Hallman, "Steady Laminar Heat Transfer in a Circular Tube with Prescribed Wall Heat Flux," Applied Scientific Research, Section A, vol. 7, 1958, p. 386.
20. T.M. Hallman, "Combined Forced and Free Convection in a Vertical Tube," PhD Dissertation, Purdue University, West Lafayette, Indiana, 1958.
21. R.D. Mikesell, "The Effect of Heat Transfer on the Flow in a Horizontal Pipe," PhD Thesis, Chemical Engineering Department, University of Illinois, 1963.
22. Anon., "Resistance Welding of Nickel and High-Nickel Alloys," Technical Bulletin T-33, The International Nickel Company.

APPENDIX A

DERIVATION OF GOVERNING EQUATIONS

Equations (1) to (3) were derived from continuity, momentum and energy equations in cylindrical coordinates. Flow is considered fully-developed, and physical properties of the fluid are assumed constant except the density variation affecting the buoyancy terms. In the energy equation axial conduction, viscous dissipation and pressure terms are ignored. The equations are then further reduced with help of the stream function ψ and expressed as

$$\frac{rv_r}{v} = \frac{\partial \psi}{\partial \theta}$$

$$\frac{v_\theta}{v} = -\frac{\partial \psi}{\partial r}$$

and the parameters

$$R = \frac{r}{a} \quad ; \quad V_x = \frac{v_x}{v/a} \quad ; \quad T^* = \frac{T_w - T}{A a Pr}$$

With these parameters the dimensionless numbers become

$$Re = -Ca^3/(4\rho v^2)$$

$$Gr = \beta g A a^4 / v^2$$

$$Pr = c_p \mu / k$$

$$Ra = Gr Pr$$

APPENDIX B

LOCATION OF TEST SECTION THERMOCOUPLES

Thermo- couple Number	Distance from Test Section Inlet [in]	Distance in Diam- eters	Location on circum- ference
57	1	4	top
59	1	4	bottom
60	2	8	top
61	3	13	top
62	4	17	top
63	5	22	top
64	6	26	top
65	7	30	top
66	8	35	top
67	9	39	top
68	10	43	top
69	11	48	top
70	12	52	top
71	12	52	side
72	12	52	bottom
73	24	104	top
74	24	104	side
75	24	104	bottom
76	36	157	top

Thermo- couple Number	Distance from Test Section Inlet [in]	Distance in Diam- eters	Location on circum- ference
77	36	157	side
78	36	157	bottom
79	48	209	top
80	48	209	side
81	48	209	bottom
82	60	261	top
83	60	261	bottom
84	60	261	side
85	66	287	top
86	68	296	top
87	20	87	top
88	70.5	307	top
89	70.5	307	side
90	70.5	307	bottom
91	16	70	top

APPENDIX C

SAMPLE CALCULATION

The data of run number 3 are chosen for purposes of illustration. The measured quantities are

Flow rate 41.6 ccm/min at 15°C

Power input 25.0 watts

Temperature distribution as given in Fig. 15 (p.33)

The heat flux was calculated from the bulk temperature rise and flow rate. The temperatures given in Fig. 15, were obtained using the thermocouple calibration results. A mean outside wall temperature was calculated from the three thermocouples placed at different circumferential locations (Fig. 12, p.24). The mean wall temperature is faired by a straight line, and shows that maximum deviation is very small.

The bulk temperature was measured before the test section inlet and after the test section exit, and its gradient assumed to be constant since the uniformity of heat generation over the tube length could not be checked.

The flow was considered fully-developed away from the region of steep temperature gradient. For this run, this occurred approximately at $X/D = 75$. At the location $X/D = 104$, the recorded mean wall and bulk

temperature were

$$T = 59.8^{\circ}\text{F}$$

$$T = 57.0^{\circ}\text{F}$$

The heat transfer coefficient is based on inner wall temperature, and the temperature drop through the wall was calculated from

$$T = \frac{W}{2k_w} \left\{ \frac{R^2 - r^2}{2} - R^2 \ln \frac{R}{r} \right\} \quad (\text{C-1})$$

where

W heat generation rate per unit volume of tube material

k_w thermal conductivity of wall ($k_w = 8.67 \text{ BTU/hr } ^{\circ}\text{F ft [22]}$)

R outside radius = 0.125 inch

r inside radius = 0.115 inch

For this apparatus (C-1) reduces to

$$T = 4.19 \cdot 10^{-4} P \quad (\text{C-2})$$

where P is test section power input in watts.

Equation (C-1) was derived with the assumption of uniform power density in the tube wall and no heat loss at the outer surface. Furthermore, a uniform axial temperature gradient in the tube wall and constant physical properties of the tube were assumed. The maximum calculated temperature drop across the tube wall was 0.24°F , and for this run was about 0.01°F .

Heat Transfer Coefficient and Nusselt Number

The Nusselt number is defined as

$$Nu = \frac{hD}{k_f} \quad (C-3)$$

where h stands for the heat transfer coefficient,

$$h = \frac{q}{T_w - T} \quad (C-4)$$

and q is the heat flow rate. The thermal conductivity of water k_f was based on the bulk temperature.

The heat flux was calculated from the flow rate and the bulk temperature rise

$$q = \dot{m} c_p \Delta T$$

where

\dot{m} mass flow rate

c_p specific heat of bulk temperature

ΔT bulk temperature gradient

Area surface area per foot length.

Therefore the heat flux and Nusselt number are

$$q = 0.061 \text{ BTU/ft}^2\text{sec}$$

$$Nu = 4.52$$

Reynolds Number

The Reynolds number is defined as

$$Re = \frac{\bar{u}D}{\nu} \quad \text{or} \quad \frac{\dot{m}}{\rho} \frac{4}{\pi \nu D} \quad (C-5)$$

if the mean velocity \bar{u} is expressed in terms of the flow rate so that for this case

$$Re = 129$$

The viscosity was evaluated at water bulk temperature.

Grashof Number

The Grashof number is here defined as

$$Gr = \frac{\beta g \Delta T D^3}{\nu^2} \quad (C-6)$$

where

β coefficient of thermal expansion

g gravitational acceleration

ΔT temperature difference between bulk fluid
and inner wall, as calculated

For this point

$$Gr = 309$$

APPENDIX D

ERROR ESTIMATES

To give some idea of the accuracy of the data, error estimates were performed. The accuracy varied a great deal between runs and for various positions on the test section. Because of the number of variables which affect the results, it is impractical to present estimated errors for each data point, and error estimates for only two cases are presented below.

Error in mass flow rate

$$0.5\% < \dot{m} < 1.5\%$$

Possible error in water temperature at inlet to test section

$$0.25^{\circ}\text{F} < T < 0.5^{\circ}\text{F}$$

Possible error in water temperature at exit of test section

$$0.5^{\circ}\text{F} < T < 1.0^{\circ}\text{F}$$

Error in tube wall temperature measurements for heated section

$$T_w = 0.25^{\circ}\text{F}$$

The errors in water temperature are noticed by slight fluctuation of the measured temperature. They are due to the error in temperature measurements and due to the inherent instability of the flow system as well as the power generation. Possible errors in property values such as thermal

conductivity and viscosity due to error in temperature may be as much as 0.2%.

Probable Errors for Results

For run number 3

Difference from wall to bulk temperature $\Delta T = 2.75^\circ\text{F}$

Axial temperature gradient of fluid bulk $A = 2.42^\circ\text{F/ft}$

From error in wall and bulk temperature
the bulk temperature gradient may be in
error of

3.4%

Error in temperature difference

$T = 0.5^\circ\text{F}$

= 15.2%

Probable error of dimensionless numbers are

$$\text{Re} = \frac{\dot{m} D}{\rho v D} = 2.0\%$$

$$\text{Gr} = \frac{\beta g \Delta T D^3}{\nu^2} = 18.5\%$$

$$\text{Nu} = \dot{m} c_p A \frac{1}{\text{Area}} \frac{1}{\Delta T} \frac{D}{k_f} = 18.5\%$$

Error estimated for run number 27

At location $X/D = 200$ the temperature difference
is

$T = 19.7^\circ\text{F}$

and the bulk temperature gradients is

$A = 3.54^\circ\text{F/ft}$

Error of different components are

mass flow rate	0.5%
wall temperature	0.25°F
fluid bulk temperature at inlet	0.25°F
fluid bulk temperature at exit	1.0°F
temperature difference	1.25°F = 6.35%
bulk temperature gradient	= 4.7%

And the error of dimensionless numbers are

Nusselt number	7.95%
Reynolds number	1.8%
Grashof number	6.35%

APPENDIX E

TABULATED LOCAL HEAT TRANSFER DATA

Run Number 1, $Q = 0.146$ BTU/sft sec

X	Nu	Re	Pr	Gr	Ra
1	8.6	347	8.8	316	2767
3	7.4	350	8.7	384	3339
5	6.3	352	8.6	465	4021
7	6.0	349	8.7	460	4017
9	5.9	356	8.5	526	4483
12	6.0	357	8.5	527	4473
24	5.2	366	8.2	702	5766
36	5.5	376	7.9	770	6108
48	5.6	387	7.7	850	6524
60	5.9	399	7.4	915	6794
70.5	6.2	409	7.2	965	6975

TABULATED LOCAL HEAT TRANSFER DATA

Run Number 2, $Q = 0.121$ BTU/sft sec

X	Nu	Re	Pr	Gr	Ra
1	8.1	124	8.8	275	2413
3	6.3	126	8.7	381	3304
5	5.5	127	8.6	457	3907
7	5.3	129	8.4	506	4277
9	4.9	130	8.3	583	4858
12	4.9	132	8.2	634	5187
24	4.8	141	7.6	867	6563
36	4.8	151	7.0	1146	8050
48	4.7	161	6.5	1470	9593
60	4.7	171	6.1	1847	11214
70.5	4.7	180	5.7	2203	12637

TABULATED LOCAL HEAT TRANSFER DATA

Run Number 3, $Q = 0.061$ BTU/sft sec

X	Nu	Re	Pr	Gr	Ra
1	8.1	120	9.1	117	1061
3	6.2	121	9.0	159	1429
5	5.0	122	8.9	206	1840
7	4.8	123	8.9	225	1987
9	4.8	124	8.8	235	2063
12	4.8	125	8.7	248	2154
24	4.5	129	8.4	309	2592
36	4.4	133	8.0	378	3039
48	4.6	137	7.7	423	3277
60	4.6	142	7.5	488	3637
70.5	4.5	146	7.2	549	3963

TABULATED LOCAL HEAT TRANSFER DATA

Run Number 11, $Q = 0.394$ BTU/sft sec

X	Nu	Re	Pr	Gr	Ra
1	9.8	534	8.4	943	7873
3	7.2	538	8.3	1336	11049
5	6.4	543	8.2	1578	12906
7	6.1	547	8.1	1724	13955
9	5.9	552	8.0	1850	14831
12	5.4	559	7.9	2135	16844
24	5.7	590	7.4	2542	18882
36	6.3	621	7.0	2861	20030
48	6.9	654	6.6	3155	20837
60	7.8	687	6.2	3358	20939
70.5	8.6	716	5.9	3478	20680

TABULATED LOCAL HEAT TRANSFER DATA

Run Number 12, $Q = 0.527$ BTU/sq sec

X	Nu	Re	Pr	Gr	Ra
1	10.4	540	8.3	1209	10032
3	8.2	546	8.2	1627	13323
5	7.4	552	8.1	1916	15463
7	6.6	558	8.0	2274	18108
9	6.3	565	7.9	2498	19617
12	6.3	571	7.8	2644	20503
24	6.3	616	7.1	3629	25805
36	6.9	659	6.6	4301	28299
48	7.6	705	6.1	4884	29781
60	8.6	750	5.7	5397	30659
70.5	9.6	788	5.4	5688	30566

TABULATED LOCAL HEAT TRANSFER DATA

Run Number 13, $Q = 0.479$ BTU/sft sec

X	Nu	Re	Pr	Gr	Ra
1	13.1	1008	8.7	695	6064
3	9.3	1015	8.7	1017	8815
5	8.3	1020	8.6	1169	10062
7	7.7	1025	8.6	1296	11092
9	7.3	1031	8.5	1409	11982
12	7.0	1038	8.4	1550	13051
24	6.2	1070	8.1	2046	16582
36	5.8	1104	7.8	2547	19884
48	5.7	1141	7.5	2959	22251
60	5.7	1179	7.2	3431	24859
70.5	5.7	1212	7.0	3833	26936

TABULATED LOCAL HEAT TRANSFER DATA

Run Number 14, $Q = 0.474$ BTU/sft sec

X	Nu	Re	Pr	Gr	Ra
1	15.9	1000	8.8	540	4758
3	9.9	1007	8.7	899	7863
5	8.6	1014	8.7	1074	9329
7	7.9	1021	8.6	1209	10425
9	7.5	1026	8.6	1307	11199
12	7.4	1032	8.5	1378	11707
24	6.7	1063	8.1	1788	14629
36	6.2	1097	7.9	2262	17823
48	5.7	1133	7.6	2818	21398
60	5.3	1171	7.3	3472	25405
70.5	5.1	1202	7.1	4083	28995

TABULATED LOCAL HEAT TRANSFER DATA

Run Number 17, $Q = 0.502$ BTU/sft sec

X	Nu	Re	Pr	Gr	Ra
1	16.1	1425	8.9	546	4846
3	12.4	1430	8.8	721	6375
5	10.7	1433	8.8	842	7426
7	8.4	1448	8.7	1138	9937
9	8.0	1455	8.7	1226	10648
12	7.5	1465	8.6	1348	11625
24	6.8	1496	8.4	1696	14224
36	6.3	1530	8.2	2066	16846
48	5.8	1565	7.9	2489	19732
60	5.4	1602	7.7	2964	22873
70.5	5.2	1634	7.5	3408	25709

TABULATED LOCAL HEAT TRANSFER DATA

Run Number 27, $Q = 0.720$ BTU/sft sec

X	Nu	Re	Pr	Gr	Ra
1	12.2	1259	6.7	3057	20618
3	9.6	1269	6.7	4005	26773
5	8.7	1278	6.6	4567	30254
12	8.0	1312	6.4	5465	35117
24	7.2	1374	6.1	7129	43470
36	7.3	1437	5.8	8134	47133
48	7.2	1497	5.5	9480	52503
60	8.0	1559	5.3	9699	51261
70.5	8.5	1611	5.1	10421	53039

TABULATED LOCAL HEAT TRANSFER DATA

Run Number 29, $Q = 0.996$ BTU/sft sec

X	Nu	Re	Pr	Gr	Ra
1	15.5	1102	8.1	1734	13989
3	10.8	1114	8.0	2625	20900
5	9.5	1126	7.9	3116	24504
7	8.9	1138	7.8	3525	27381
9	8.5	1151	7.7	3853	29553
12	8.2	1171	7.5	4309	32418
24	7.7	1252	7.0	5960	41601
36	7.9	1332	6.5	7353	47765
48	8.1	1417	6.1	8896	53839
60	8.3	1501	5.7	10545	59789
70.5	8.5	1571	5.4	11954	64383

TABULATED LOCAL HEAT TRANSFER DATA

Run Number 31, $Q = 0.754$ BTU/sft sec

X	Nu	Re	Pr	Gr	Ra
1	15.3	1583	8.2	1223	10069
3	12.0	1591	8.2	1608	13147
5	9.7	1599	8.1	2039	16559
7	9.0	1608	8.1	2254	18188
9	8.7	1616	8.0	2385	19112
12	8.5	1631	7.9	2569	20357
24	8.8	1689	7.6	2876	21915
36	8.8	1749	7.3	3367	24653
48	8.4	2037	6.1	6166	37935
60	8.5	1872	6.8	4524	30692
70.5	8.0	1926	6.6	5328	34981

TABULATED LOCAL HEAT TRANSFER DATA

Run Number 32, $Q = 0.989$ BTU/sft sec

X	Nu	Re	Pr	Re	Ra
1	11.5	1600	8.2	2218	18103
3	10.8	1606	8.1	2406	19541
5	9.5	1614	8.1	2816	22724
7	8.8	1625	8.0	3119	24958
9	8.5	1634	8.0	3329	26469
12	8.8	1658	7.9	3437	26862
24	8.0	1734	7.4	4581	34021
36	9.9	1815	7.0	4445	31367
48	9.0	1903	6.7	4395	29380
60	8.2	1977	6.4	7353	47034
70.5	8.1	2045	6.1	8383	51582

TABULATED LOCAL HEAT TRANSFER DATA

Run Number 34, $Q = 0.254$ BTU/sft sec

X	Nu	Re	Pr	Gr	Ra
1	9.0	1577	8.2	699	5755
3	8.6	1581	8.2	746	6121
5	8.3	1585	8.2	782	6391
7	8.2	1587	8.2	800	6528
9	7.9	1589	8.1	831	6769
12	7.9	1592	8.1	839	6819
24	7.2	1609	8.0	970	7777
36	6.6	1628	7.9	1125	8903
48	6.3	1646	7.8	1233	9626
60	6.5	1666	7.7	1268	9772
70.5	6.9	1685	7.6	1252	9523

TABULATED LOCAL HEAT TRANSFER DATA

Run Number 35, $Q = 0.231$ BTU/sft sec

X	Nu	Re	Pr	Gr	Ra
1	10.8	1106	8.1	564	4570
3	9.7	1109	8.1	637	5148
5	9.1	1112	8.1	686	5523
7	8.6	1115	8.0	736	5905
9	8.2	1117	8.0	786	6294
12	7.9	1120	8.0	825	6580
24	6.6	1137	7.8	1064	8341
36	5.9	1155	7.7	1268	9772
48	5.7	1173	7.6	1409	10671
60	5.8	1191	7.4	1471	10946
70.5	6.4	1210	7.3	1415	10342

TABULATED LOCAL HEAT TRANSFER DATA

Run Number 36, $Q = 0.258$ BTU/sft sec

X	Nu	Re	Pr	Gr	Ra
1	11.1	1073	8.3	546	4551
3	10.0	1075	8.3	612	5085
5	9.3	1078	8.3	668	5533
7	9.0	1081	8.3	701	5791
9	8.4	1083	8.2	759	6255
12	8.3	1088	8.2	789	6458
24	7.1	1107	8.0	1012	8111
36	6.4	1124	7.9	1212	9530
48	6.3	1143	7.7	1323	10215
60	6.7	1164	7.6	1349	10201
70.5	7.3	1181	7.4	1307	9724

TABULATED LOCAL HEAT TRANSFER DATA

Run Number 37, $Q = 0.500$ BTU/sft sec

X	Nu	Re	Pr	Gr	Ra
1	12.4	1085	8.3	956	7946
3	9.4	1088	8.3	1277	10577
5	8.9	1090	8.3	1379	11385
7	8.0	1093	8.2	1556	12809
12	7.8	1116	8.0	1766	14155
24	6.6	1156	7.7	2456	18895
36	6.5	1195	7.4	2850	21130
48	6.2	1235	7.1	3462	24734
60	7.4	1275	6.9	3284	22635
70.5	7.6	1311	6.7	3579	23891

TABULATED LOCAL HEAT TRANSFER DATA

Run Number 38, $Q = 0.497$ BTU/sft sec

X	Nu	Re	Pr	Gr	Ra
1	11.3	656	8.3	1049	8720
3	8.6	660	8.2	1445	11873
5	8.2	656	8.1	1571	12780
7	7.5	672	8.0	179	14441
9	7.1	678	8.0	1994	15855
12	6.9	687	7.8	2186	17114
24	6.9	726	7.4	2784	20480
36	6.8	757	7.0	3317	23258
48	7.6	807	6.5	3768	24585
60	8.0	849	6.1	4262	26220
70.5	8.4	885	5.9	4678	27464

TABULATED LOCAL HEAT TRANSFER DATA

Run Number 39, $Q = 0.972$ BTU/sft² sec

X	Nu	Re	Pr	Gr	Ra
1	9.9	662	8.2	2427	20012
3	8.5	673	8.1	3094	24961
5	7.9	685	7.9	3603	28471
7	7.6	696	7.8	4042	31351
9	7.3	709	7.6	4540	34484
12	7.7	728	7.4	4817	35486
24	8.0	808	6.5	6973	45647
36	8.2	893	5.8	9517	55567
48	8.6	976	5.3	12221	64500
60	9.0	1065	4.8	15282	73061
70.5	9.3	1138	4.4	18064	80018

TABULATED LOCAL HEAT TRANSFER DATA :

Run Number 43, $Q = 0.234$ BTU/sft sec

X	Nu	Re	Pr	Gr	Ra
1	8.0	331	8.3	703	5826
3	6.5	334	8.2	906	7434
5	5.9	336	8.1	1035	8406
7	5.6	339	8.0	1145	9212
9	5.5	342	8.0	1207	9609
12	5.4	346	7.8	1304	10232
24	5.6	364	7.4	1571	11628
36	5.9	383	7.0	1829	12787
48	6.2	403	6.6	2086	13789
60	6.6	422	6.3	2340	14630
70.5	7.0	440	6.0	2523	15076

TABULATED LOCAL HEAT TRANSFER DATA

Run Number 44, $Q = 0.440$ BTU/sft sec

X	Nu	Re	Pr	Gr	Ra
1	9.8	335	8.2	1143	9363
3	7.7	340	8.1	1558	12548
5	6.6	344	7.9	1923	15263
7	6.3	349	7.8	2140	16728
9	6.0	354	7.7	2376	18281
12	6.2	366	7.4	2664	19733
24	6.4	401	6.7	3731	24859
36	6.5	439	6.0	5044	30308
48	6.6	477	5.5	6521	35717
60	6.7	516	5.0	8264	41325
70.5	6.9	550	4.6	9775	45448

TABULATED LOCAL HEAT TRANSFER DATA

Run Number 45, $Q = 0.646$ BTU/sft sec

X	Nu	Re	Pr	Gr	Ra
1	7.9	325	8.1	2188	17656
3	7.2	333	7.9	2699	21192
5	6.9	340	7.6	3120	23849
7	6.9	349	7.4	3465	25775
9	6.8	357	7.2	3867	28012
12	6.6	372	6.9	4618	32028
24	6.5	427	5.9	7703	45568
36	6.4	482	5.1	11679	60051
48	6.4	543	4.5	16714	75226
60	6.4	603	4.0	22745	90569
70.5	6.5	654	3.6	28120	101948

TABULATED LOCAL HEAT TRANSFER DATA

Run Number 46, $Q = 0.642$ BTU/sft sec

X	Nu	Re	Pr	Gr	Ra
1	9.1	378	6.8	3661	24730
3	7.6	387	6.6	4741	31223
5	7.0	396	6.4	5582	35820
7	6.7	404	6.3	6289	39326
9	6.7	413	6.1	6805	41497
12	7.0	429	5.8	7375	43126
24	6.8	484	5.1	11182	56983
36	6.8	543	4.4	15940	71191
48	6.9	604	4.0	21700	85424
60	7.0	664	3.5	27718	98218
70.5	7.1	715	3.3	33303	108565